

# The anatomy of the Late Miocene baleen whale *Cetotherium riabinini* from Ukraine

PAVEL GOL'DIN, DMITRY STARTSEV, and TATIANA KRAKHMALNAYA



Gol'din, P., Startsev, D., and Krakhmalnaya, T. 2014. The anatomy of the Late Miocene baleen whale *Cetotherium riabinini* from Ukraine. *Acta Palaeontologica Polonica* 59 (4): 795–814.

We re-describe *Cetotherium riabinini*, a little-known baleen whale from the Late Miocene of the Eastern Paratethys represented by an exceptionally well-preserved skull and partial skeleton. *C. riabinini* is shown to be closely related to *C. rathkii*, the only other member of the genus. Cetotheriids from the Eastern Paratethys are remarkable for their pachyosteosclerotic postcranial skeleton, and are among the youngest known cetaceans displaying this morphology. *C. riabinini* likely followed a generalised feeding strategy combining herpetocetine-like continuous suction feeding, as seen in the mallard *Anas platyrhynchos*, and eschrichtiid-like intermittent suction feeding. This hypothesis may explain the mechanism and function of cranial kinesis in baleen whales. Many characteristics of the mysticete skull likely evolved as a result of cranial kinesis, thus leading to multiple instances of morphological convergence across different phylogenetic lineages.

**Key words:** Cetacea, Mysticeti, Cetotheriidae, pachyosteosclerosis, suction feeding, cranial kinesis, Miocene, Paratethys, Ukraine.

Pavel Gol'din [pavelgoldin412@gmail.com], Taurida National University, 4, Vernadsky Avenue, Simferopol, Crimea, 95007 Ukraine; current address: Department of Natural History and Palaeontology, The Museum of Southern Jutland, Lergravsvej 2, 6510, Gram, Denmark;

Dmitry Startsev [dbstarcev@gmail.com], Taurida National University, 4, Vernadsky Avenue, Simferopol, Crimea, 95007 Ukraine;

Tatiana Krakhmalnaya [tv\_krakhm@mail.ru], Academician V.A. Topachevsky Paleontological Museum of the National Museum of Natural History of the National Academy of Sciences of Ukraine, 15, Bohdan Khmelnytsky St., Kiev, 01601 Ukraine.

Received 14 September 2012, accepted 6 March 2013, available online 13 March 2013.

Copyright © 2014 P. Gol'din et al. This is an open-access article distributed under the terms of the Creative Commons Attribution License, which permits unrestricted use, distribution, and reproduction in any medium, provided the original author and source are credited.

## Introduction

*Cetotherium*, the type genus of the mysticete family Cetotheriidae, was described in 1843 based on its type and only known species, *Cetotherium rathkii*, itself known from just a single partial skull from the late Sarmatian (Late Miocene) of the southern part of the Taman Peninsula (north-western Caucasus, Russia; Fig. 1) (Rathke 1835; Brandt 1843, 1873). For decades, Cetotheriidae was used as a wastebasket taxon for dozens of possibly unrelated fossil mysticetes. However, recent work redefined the family as a smaller, monophyletic group of species related to *Cetotherium* (Cetotheriidae sensu stricto; Bouetel and Muizon 2006; Steeman 2007; Whitmore and Barnes 2008). Hereafter, the term Cetotheriidae is used in this sense.

Cetotheriids are known from the Neogene of the Atlantic, Pacific and Eastern Paratethys, but none except *C. rathkii* clearly belong to genus *Cetotherium*. In 1930, a well-pre-

served skull and associated partial skeleton (Fig. 2) was found near Nikolaev, south Ukraine (Fig. 1), and briefly described by Hofstein (1948, 1965) as *C. riabinini*. Here we re-describe *C. riabinini*, place it in a phylogenetic context, and discuss its implications for the diagnoses of *Cetotherium* and Cetotheriidae. In addition, we suggest a potential feeding strategy, based on the presence of rostral kinesis in this species.

**Institutional abbreviations.**—NMNH-P, Academician V.A. Topachevsky Paleontological Museum of the National Museum of Natural History of the National Academy of Sciences of Ukraine, Kiev, Ukraine; ONU, Zoological Museum of I.I. Mechnikov Odessa National University, Odessa, Ukraine; PIN, A.A. Borisyak Paleontological Institute, Russian Academy of Sciences, Moscow, Russia; VMNH, Virginia Museum of Natural History, Martinsville, Virginia, USA.

**Other abbreviations.**—C, cervical; Ca, caudal; T, thoracic; L, lumbar.

## Material and methods

Measurements of the specimen are provided in Tables 1–4. With the exception of the mandibles, measurements of paired or bilaterally symmetrical structures were taken on the left side. Skeletal terminology generally follows Mead and Fordyce (2009) and muscular terminology is based on Lambertsen et al. (1995).

We performed a phylogenetic analysis based on the matrix of Marx (2011), excluding *Aulocetus latus* Kellogg, 1940, but including *Joumocetus shimizui* Kimura and Hasegawa, 2010, *Cetotherium rathkii* and *Cetotherium riabinini* (Supplementary Online Material, SOM available at [http://app.pan.pl/SOM/app59-Goldin\\_et\\_al\\_SOM.pdf](http://app.pan.pl/SOM/app59-Goldin_et_al_SOM.pdf)). Heuristic parsimony analysis of the matrix was performed using the “traditional search” option of TNT v. 1.1 (Goloboff et al. 2003) using 10 000 replicates (saving 10 trees per replicate), and the results summarised in a strict consensus tree with zero-length branches collapsed. Branch support was estimated using bootstrap resampling, based on 1000 replicates.

## Geological setting

According to Hofstein (1948, 1965), *Cetotherium riabinini* was found in the outskirts (“okolytsi”) of the City of Nikolaev in southern Ukraine, but the precise locality is unfortunately unknown (even in 1930, Nikolaev occupied a vast area along the Southern Bug River). The specimen was found in late Sarmatian limestone (Hofstein 1948, 1965), which likely corresponds to the widely distributed Chersonian Formation and generally correlates with the early Tortonian (Neveskaya et al. 2003; Radionova et al. 2012). Although Hofstein (1948) did not provide any data to justify his age estimate, outcrops exposing the Chersonian Formation are common in Nikolaev, and we have no reasons to dispute his assessment. Note that the upper boundary of the Sarmatian (sensu lato) of the Eastern Paratethys has been dated to as late as 9.3 Ma (Neveskaya et al. 2003) or even younger (Radionova et al. 2012), and should not be confused with the older, Middle Miocene Sarmatian sensu stricto of the Central Paratethys.



Fig. 1. Map of the Black Sea region showing the type localities of *Cetotherium riabinini* and *Cetotherium rathkii*.

## Systematic palaeontology

Cetacea Brisson, 1762

Mysticeti Gray, 1864

Family Cetotheriidae Brandt, 1872

*Included genera:* *Cetotherium* Brandt, 1843; *Cephalotropis* Cope, 1896; *Eucetotherium* Kellogg, 1931; *Herpetocetus* Van Beneden, 1872; *Joumocetus* Kimura and Hasegawa, 2010; *Kurdalagonus* Tarasenko and Lopatin, 2012; *Metopocetus* Cope, 1896; *Mixocetus* Kellogg, 1934a; *Nannocetus* Kellogg, 1929; *Piscobalaena* Pilleri and Siber, 1989.

*Emended diagnosis* (modified from Bouetel and Muizon 2006).—Toothless mysticetes characterised by (i) strongly telescoped facial bones, with the anterior margin of the nasal located at or posterior to the level of the antorbital notch, the ascending processes of the maxilla extending posteriorly to the level of the postorbital process of the frontal, and the combined posterior edges of the nasal, premaxilla and maxilla being wedge-shaped and extending almost to the tip of the occipital shield (X-shaped vertex); (ii) ascending processes of the maxillae with concave lateral margins (in dorsal view), contacting medially or approximating each other at



Fig. 2. Mounted skeleton of the cetotheriid baleen whale *Cetotherium riabinini* Hofstein, 1948, Late Miocene of Nikolaev, Ukraine, NMNH-P 668/1, in lateral view.

their posterior apices; (iii) a dorsoventrally thickened distal portion of the lateral process of the maxilla; (iv) a distally widened supraorbital process of the frontal; (v) a shallow glenoid fossa; (vi) a supraoccipital shield extending no further anteriorly than the line joining the postorbital processes of the frontals; (vii) a paroccipital process extending posterior to the posterior edge of the occipital condyle in dorsal view; (viii) a transversely narrow sigmoid process of the tympanic bulla lacking an inflated base; (ix) a well-developed anterior process and lateral tuberosity of the periotic; (x) a short posterior process of the tympanoperiotic with a flattened distal surface broadly exposed on the posterolateral wall of the skull; and (xi) a mandible having an angular process extending posterior to the condyle, a condyle oriented obliquely to the long axis of the body, and a small and laterally bent coronoid process.

**Remarks.**—Our diagnosis of Cetotheriidae is based on several recent phylogenetic analyses (Bouetel and Muizon 2006; Steeman 2007; Marx 2011), the revision of a wide range of material from Belgium (Steeman 2010), and (re-) descriptions of *Herpetocetus* spp. (Whitmore and Barnes 2008), *Herpetocetinae* indet. (Boessenecker 2011), *Joumocetus shimizui* (Kimura and Hasegawa 2010) and *Kurdalagonus mchedlidzei* (Tarasenko and Lopatin 2012). *Mixocetus elysius* Kellogg, 1934a matches the diagnosis of Cetotheriidae according to points i–iv, vi, vii, x—listed here, but the poor state of preservation of the holotype raises doubts regarding its identification. Equally difficult to determine are the affinities of *Plesiocetopsis hupschii* Van Beneden, 1859, since the holotype is unavailable for study (see Steeman 2010).

*Titanocetus sammarinensis* (Capellini, 1901), “*Mesocetus*” *argillarius* Roth, 1978, *Diorocetus hiatus* Kellogg, 1968 and eschrichtiids have previously been considered to form part of, or be closely related to, cetotheres (Bisconti 2006, 2012; Steeman 2007). However, none of these taxa have a posterior process of the tympanoperiotic that is broadly exposed on the posterolateral wall of the skull. Besides cetotheres, the only mysticetes to show this feature are neobalaenids (Fitzgerald 2012): *Caperea marginata* (Gray, 1846) and *Miocaperea pulchra* Bisconti, 2012. However, the taxonomic position of neobalaenids is still controversial, and they have variously been proposed to ally with balaenids (Steeman 2007; Ekdale et al. 2011; Bisconti 2012; Churchill et al. 2012), balaenopteroids (Sasaki et al. 2005; McGowen et al. 2009; Marx 2011) or cetotheriids (e.g., Fordyce and Marx 2012; Marx et al. 2013). In addition, we note that *Caperea marginata* has a rectangular tympanic bulla in medial and lateral views, a specific trait shared by *Aglaoctetus patulus* Kellogg, 1968 and other genera included by Steeman (2007) in the family Aglaoctetidae.

### Genus *Cetotherium* Brandt, 1843

**Type species:** *Cetotherium rathkii* Brandt, 1843; south coast of Taman Peninsula; Tortonian, Late Miocene of the Eastern Paratethys.

**Included species:** Type species and *Cetotherium riabinini* Hofstein, 1948.

**Diagnosis** (Fig. 3).—Small cetotheres (3 to 4 m long; condylobasal length of skull ~1 m) differing from other members of

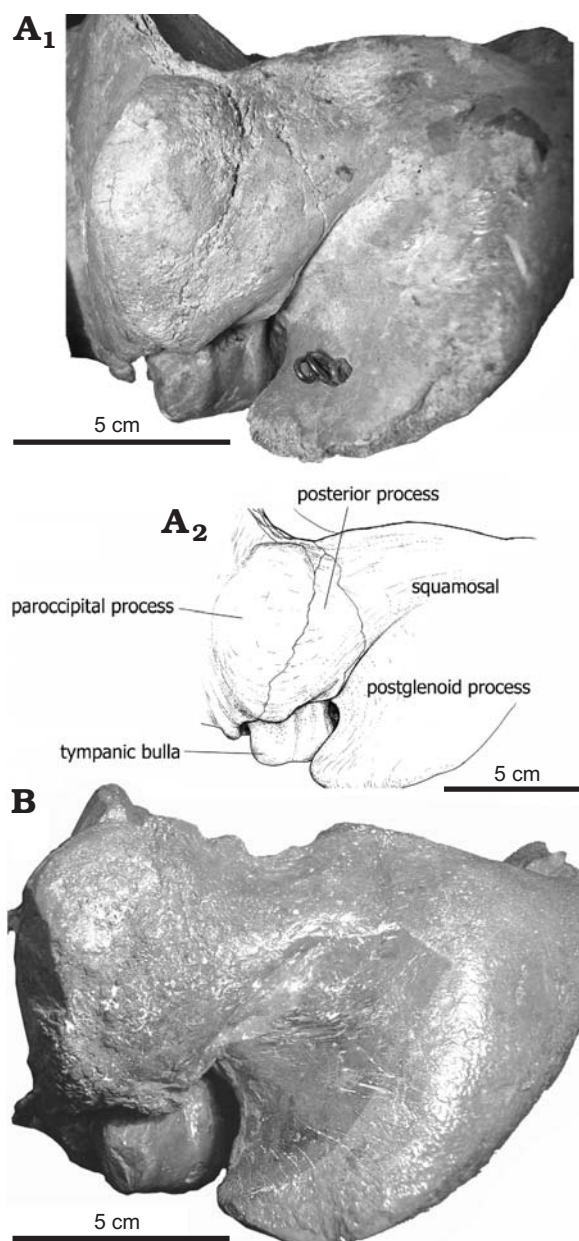


Fig. 3. Comparison of the distal surface of the composite posterior process of the tympanoperiotic in posterolateral view in two cetotheriid baleen whales. **A.** *Cetotherium riabinini* Hofstein, 1948, Late Miocene of Nikolaev, Ukraine, NMNH-P 668/1. Photograph (A<sub>1</sub>), explanatory drawing (A<sub>2</sub>). **B.** *Cetotherium rathkii* Brandt, 1843, south coast of Taman Peninsula, Tortonian, Late Miocene, PIN 1840/1; inverted.

the family in having a narrow rostrum, a roughly triangular (pointing dorsally) exposure of the posterior process of the tympanoperiotic on the posterolateral wall of the skull, a triangular occipital shield with a low and transversely wide external occipital crest, and a tympanic bulla as high and wide anteriorly as it is posteriorly; *Cetotherium* differs from all cetotheres except *Kurdalagonus* in having an anteroposteriorly short and dorsoventrally high zygomatic process of the squamosal and a transversely wide postglenoid process; differs from all cetotheres except “*Cetotherium*” *mayeri*

(sensu Riabinin 1934) in having a mandible with a straight, as opposed to laterally curved, distal portion; differs from *Herpetocetus* and *Nannocetus* in having a robust, bulbous paroccipital process; differs from *Herpetocetus*, *Metopocetus*, and *Nannocetus* in having a ventrally open (as opposed to partially floored) facial sulcus on the posterior process of the periotic; differs from all cetotheriids except *Eucetotherium helmersenii* (Brandt, 1871), *Herpetocetus*, and *Nannocetus* in having the postglenoid process oriented ventrally to ventromedially in posterior view; differs from *Herpetocetus*, *Joumocetus*, *Metopocetus*, *Nannocetus*, and *Piscobalaena* in having the proximal portion of the premaxilla not covered by the maxilla, and ascending processes of the maxillae approximating each other posteriorly without ever making contact.

*Remarks.*—*Cetotherium* has in the past been used as a wastebasket taxon for several species not belonging to this genus. In particular, the diagnoses of Brandt (1873), Spassky (1954), and Mchedlidze (1970) define a wider group including all cetotheriids.

*Geographic and stratigraphic range.*—Black Sea region; Tortonian, Late Miocene of the Eastern Paratethys.

### *Cetotherium riabinini* Hofstein, 1948

Figs. 2–16, 18 and 19.

*Type and only specimen:* NMNH-P 668/1, partial skeleton including a nearly complete skull.

*Type locality:* City of Nikolaev, southern Ukraine.

*Type horizon:* Late Sarmatian (corresponding to the early Tortonian, Late Miocene) of the Eastern Paratethys (Radionova et al. 2012).

*Diagnosis* (Fig. 4).—Species of *Cetotherium* differing from *C. rathkii* in having: (i) a triangular nasal that gradually tapers posteriorly (as opposed to being wedge-like and strongly compressed); (ii) the anterior edge of nasal located just posterior to the level of the antorbital notch (not far posterior as in *C. rathkii*); (iii) an elongated posterior portion of the facial skull; (iv) a V-shaped, notched anterior margin of the palatines; (v) an angular (as opposed to gradually curved) anterior edge of the supraorbital process of the frontal; (vi) the distal portion of the postglenoid process of the squamosal bent medially, protruding dorsally and posteriorly (not posteroventrally as in *C. rathkii*); (vii) a convex nuchal crest in dorsal view; and (viii) a sigmoid process of the tympanic bulla oriented slightly posteriorly (not perpendicularly to the long axis of the bulla as in *C. rathkii*).

### *Description*

All parts of the specimen are exceptionally well preserved, with no signs of post-depositional deformation. The skull (Figs. 2, 5–7, Table 1) is about 970 mm long, which constitutes approximately one third of the estimated total body length. In dorsal view, the rostrum is transversely narrow, triangular and gradually tapers along its entire length. In lateral view, the rostrum is straight and directed anteroventrally relative to the braincase. The unfused rostral bones have been transversely displaced, but show no signs of distortion.

Table 1. Cranial measurements (in mm) of *Cetotherium riabinini* and *Cetotherium rathkii*; e, estimated.

Measurement	<i>C. riabinini</i>	<i>C. rathkii</i>
Total skull length	970	
Condylbasal length	960	
Postglenoid length	930	
Zygomatic width	326	333
Rostrum length	720	
Length of neurocranium (measured from transverse line joining antorbital notches to the occipital condyle)	220	231e
Length of premaxilla	820	
Rostrum width at ¼ of its length	95	
Rostrum width at ½ of its length	112	
Rostrum width at ¾ of its length	144	
Distance between antorbital notches	186	165
Combined width of ascending processes of maxillae at their tips	36	31
Length of nasal	74	72
Distal width of nasal	12	10
Skull height at antorbital notch	114	
Greatest width of nares	44	33
Distance between posterior margin of nasal and anteriormost point of occipital shield	37	25
Anteroposterior length of parietal exposure on skull vertex	19	15
Skull width across lateral processes of the maxillae	258	
Skull width across preorbital processes of the frontals	246	244
Skull width across postorbital processes of the frontals	294	275e
Anteroposterior length of orbit	70	80
Minimum intertemporal width	105	
Greatest length/width of temporal fossa	58/85	58/94
Distance between tip of zygomatic process and tip of postglenoid process	144	144
Distance between posteriormost points of the paroccipital processes	200	202
Distance between tip of zygomatic process and tip of paroccipital process	154	167
Maximum distance between outer margins of nuchal crests	205	222
Width/height of foramen magnum	26e/33e	
Bicondylar width	86	
Condylar height	55	
Distance between medial margins of the foramina pseudovale	100	99
Distance between lateral margins of the basioccipital crests	75	78
Postglenoid width	185	
Greatest height of neurocranium	138	126
Greatest inner length of brain cavity	150+	108
Length of tympanic bulla	51	50
Width of tympanic bulla in ventral view	37	34e
Posterior height of tympanic bulla in medial view	25	26

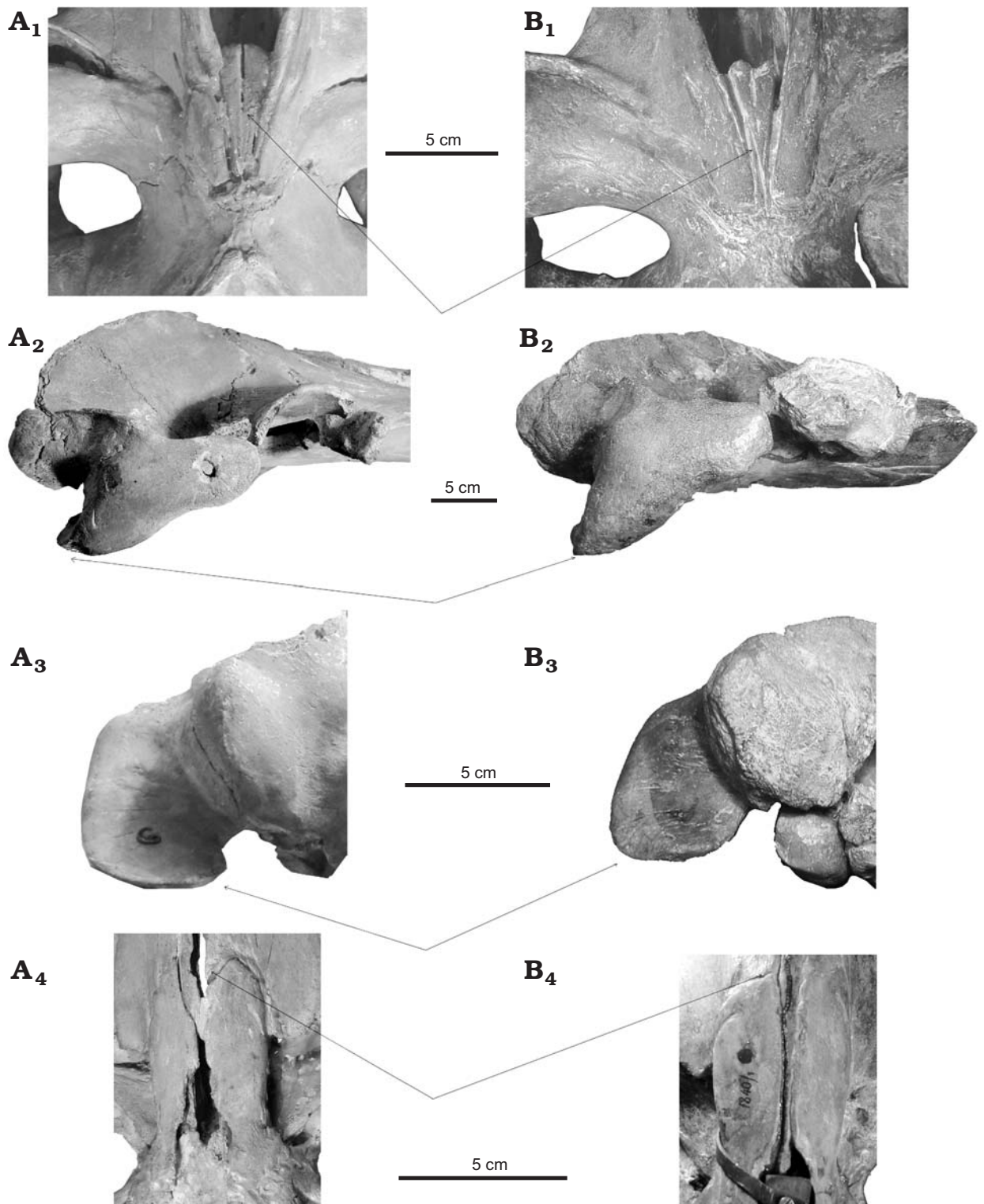


Fig. 4. Comparison of the cetotheriid baleen whales *Cetotherium riabinini* Hofstein, 1948, Late Miocene of Nikolaev, Ukraine, NMNH-P 668/1 (A) and *Cetotherium rathkii* Brandt, 1843, south coast of Taman Peninsula, Tortonian, Late Miocene, PIN 1840/1 (B). Nasals, dorsal view (A<sub>1</sub>, B<sub>1</sub>); squamosal, lateral view (A<sub>2</sub>, B<sub>2</sub>); squamosal, posterior view (A<sub>3</sub>, B<sub>3</sub>); palatines, ventral view (A<sub>4</sub>, B<sub>4</sub>). Arrows indicate diagnostic differences.

**Skull**

*Premaxilla*.—In dorsal view, the premaxilla is narrow transversely, but slightly widens near its anterior tip (Fig. 5A). In lateral view, the premaxilla is elevated above the maxilla along most of the rostrum (Fig. 5C). Anterior to the narial

fossa, its medial margin is transversely concave. Posterior to the narial fossa, the premaxillae diverge, before converging again and becoming narrow transversely at the level of the antorbital notch. The premaxilla terminates 10–15 mm anterior to the posterior margin of the nasal, possibly as a result of

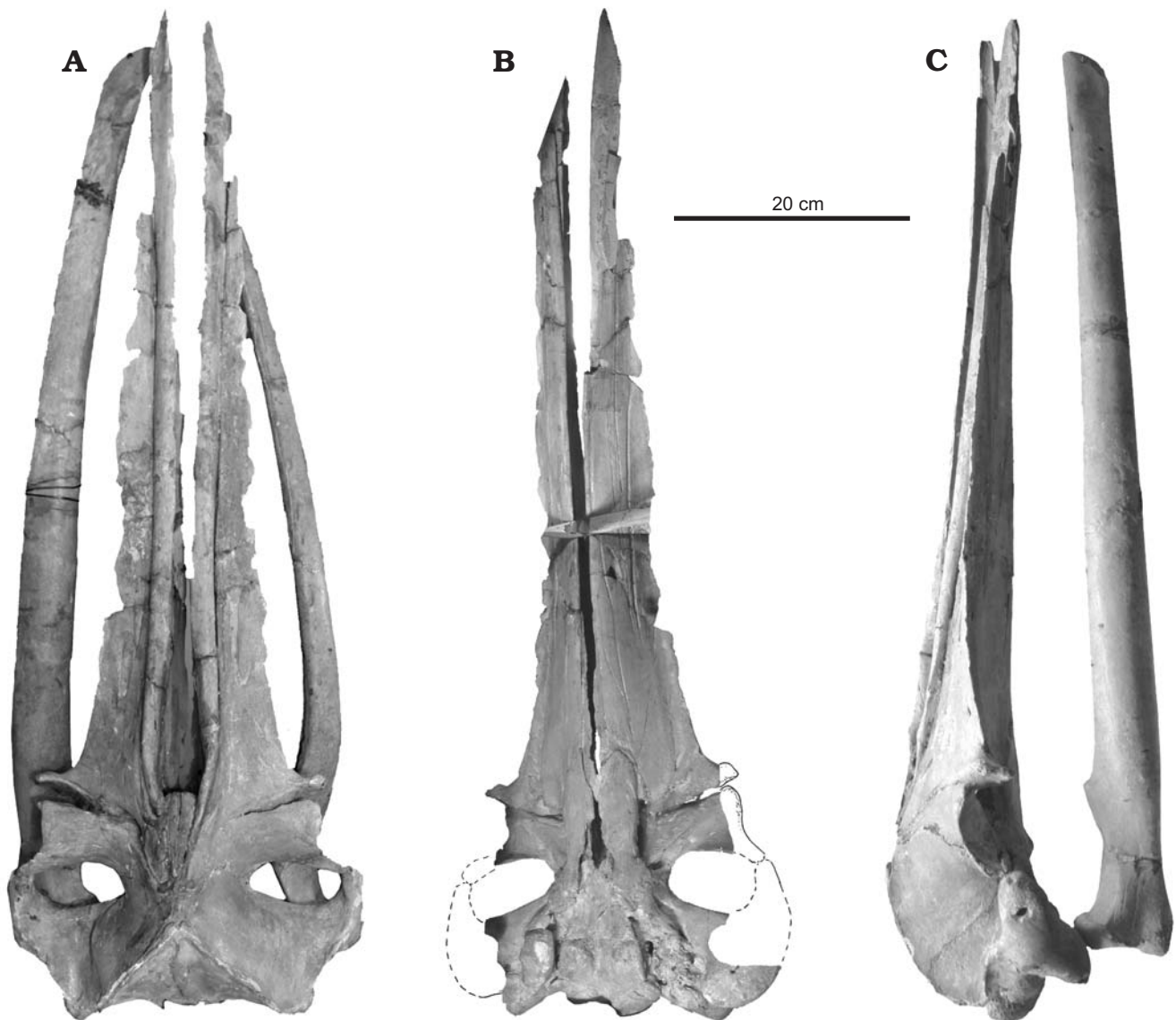


Fig. 5. Skull of the cetotheriid baleen whale *Cetotherium riabinini* Hofstein, 1948, Late Miocene of Nikolaev, Ukraine, NMNH-P 668/1, in dorsal (A), ventral (B, dashed lines indicate areas obscured by the mandibles), and lateral (C) views.

post-mortem displacement. In cross section, the premaxilla is roughly triangular along its anteriormost part, oval along the most distal portion, and transversely compressed adjacent to the bony nares.

*Maxilla*.—The maxilla is slightly arched dorsoventrally (Fig. 5C) and strongly tapers from its base to the tip of the rostrum in dorsal view (Fig. 5A, B). In ventral view, the palatine process descends ventromedially and contacts the vomer medially to form a longitudinal keel. Parallel and somewhat medial to the lateral border of the maxilla, an alveolar groove (see also Bouetel and Muizon 2006) runs along the entire length of the rostrum (Figs. 5B, 6B). Several rows of sub-parallel, anteroposteriorly oriented palatal foramina and associated sulci occur on the anterior portion of the maxilla, before becoming aligned into a single row and oriented anterolaterally near the base of the rostrum. These palatal foramina are noticeable more abundant on the left side, indicating some degree of

asymmetry. The posterior border of the infraorbital plate is interrupted by a notch located at the level of the alveolar groove.

In dorsal view, the posterior third of the maxilla bears several dorsal infraorbital foramina (12 on the left side, 8 on the right), the posteriormost of which is located at the base of ascending process (Fig. 6A). Unlike in *Piscobalaena nana*, none of the foramina stands out for being particularly large. The posterolateral margin of the maxilla is concave and terminates in a short, anteroposteriorly narrow lateral process oriented perpendicular to the longitudinal axis of the skull. At its apex, the lateral process of the maxilla is thickened dorsoventrally. Medially, it merges into the antorbital process, which runs to the base of the ascending process (Fig. 6A). The ascending process is anteroposteriorly elongate and parallel-sided, tapering only slightly anteroposteriorly. Posteriorly, the ascending processes approximate each other posterior to the nasals, but never actually come into contact.

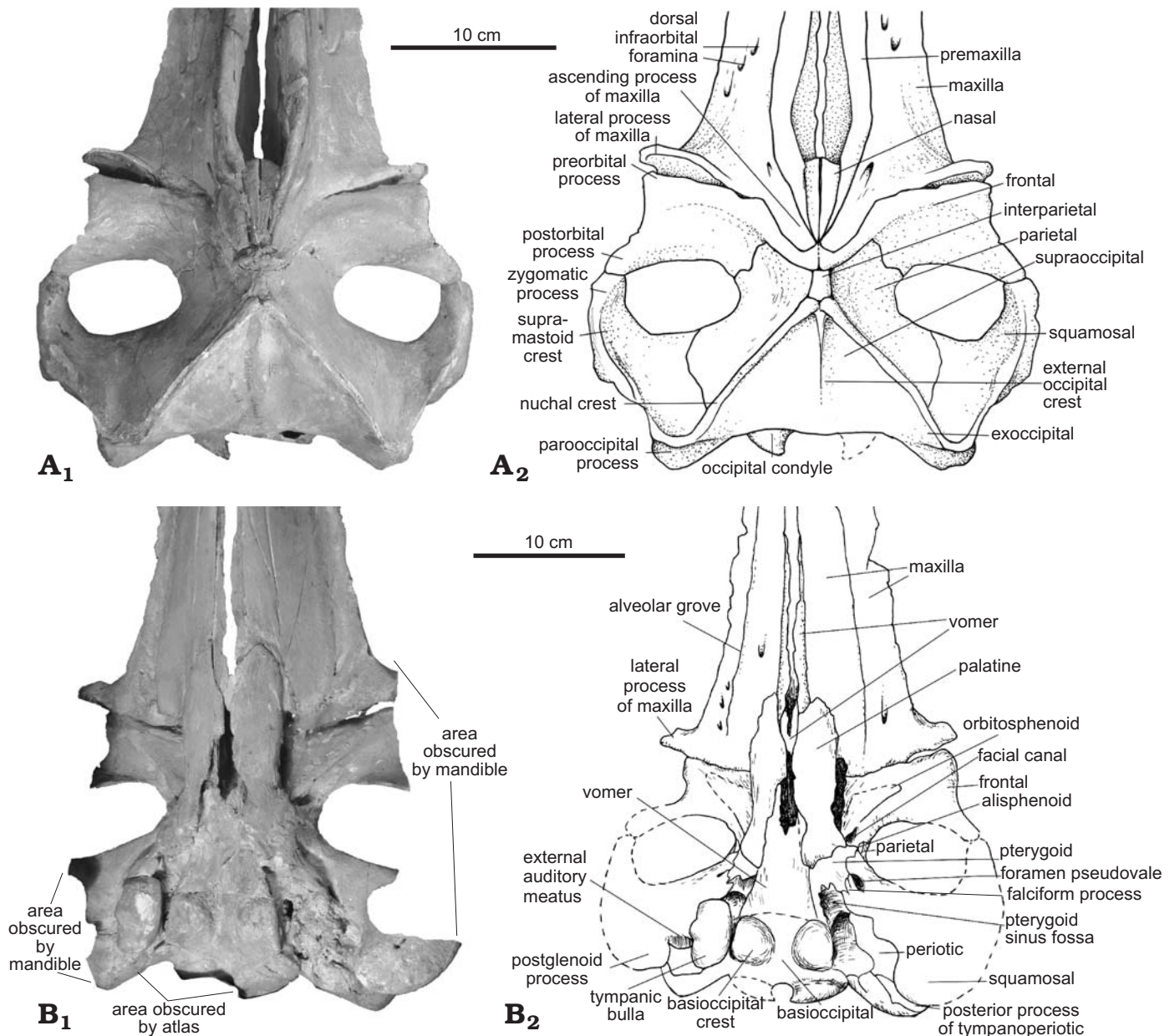


Fig. 6. Neurocranium of the cetotheriid baleen whale *Cetotherium riabinini* Hofstein, 1948, Late Miocene of Nikolaev, Ukraine, NMNH-P 668/1, in dorsal (A) and ventral (B) views. Photographs (A<sub>1</sub>, B<sub>1</sub>), explanatory drawings (A<sub>2</sub>, B<sub>2</sub>).

*Nasal*.—The nasal is triangular and gradually narrows posteriorly. Its anterior margin is located at the level of the antorbital process of the maxilla, whereas the posterior margin aligns with the base of the postorbital process of the frontal (Figs. 4A, 5A, 6A).

*Lacrimal, mesethmoid*.—Missing.

*Frontal*.—The frontal is narrowly exposed on the skull vertex, posterior to the ascending process of the maxilla (Fig. 6A). The gradually descending supraorbital process of the frontal is oriented anterolaterally, widens distally, and has an angular anteromedial margin. There is a low but noticeable transverse crest (orbitotemporal crest?) located on the anterior half of the supraorbital process (Fig. 6A), as well as second, hardly visible crest running further posteriorly. The preorbital process is

short and massive. The postorbital process is long and slender, oriented posterolaterally, and closely approximates the apex of the zygomatic process of the squamosal (Figs. 6A, 7A). The temporal fossa is oval in dorsal view and roughly 1.5 times as wide transversely as it is long anteroposteriorly. The fronto-parietal suture descends anteroventrally from the vertex and follows a zigzag pattern in lateral view (Figs. 6A, 7A).

*Parietal*.—The parietals are narrowly exposed on the vertex, where they are separated from each other by the interparietal (Fig. 6A). In lateral view, the parietal is about as long anteroposteriorly as it is high dorsoventrally, and borders the alisphenoid ventrally (Figs. 7A, 8). The parietal-squamosal suture is keeled. In lateral view, the nuchal crest is rounded and somewhat elevated dorsally.

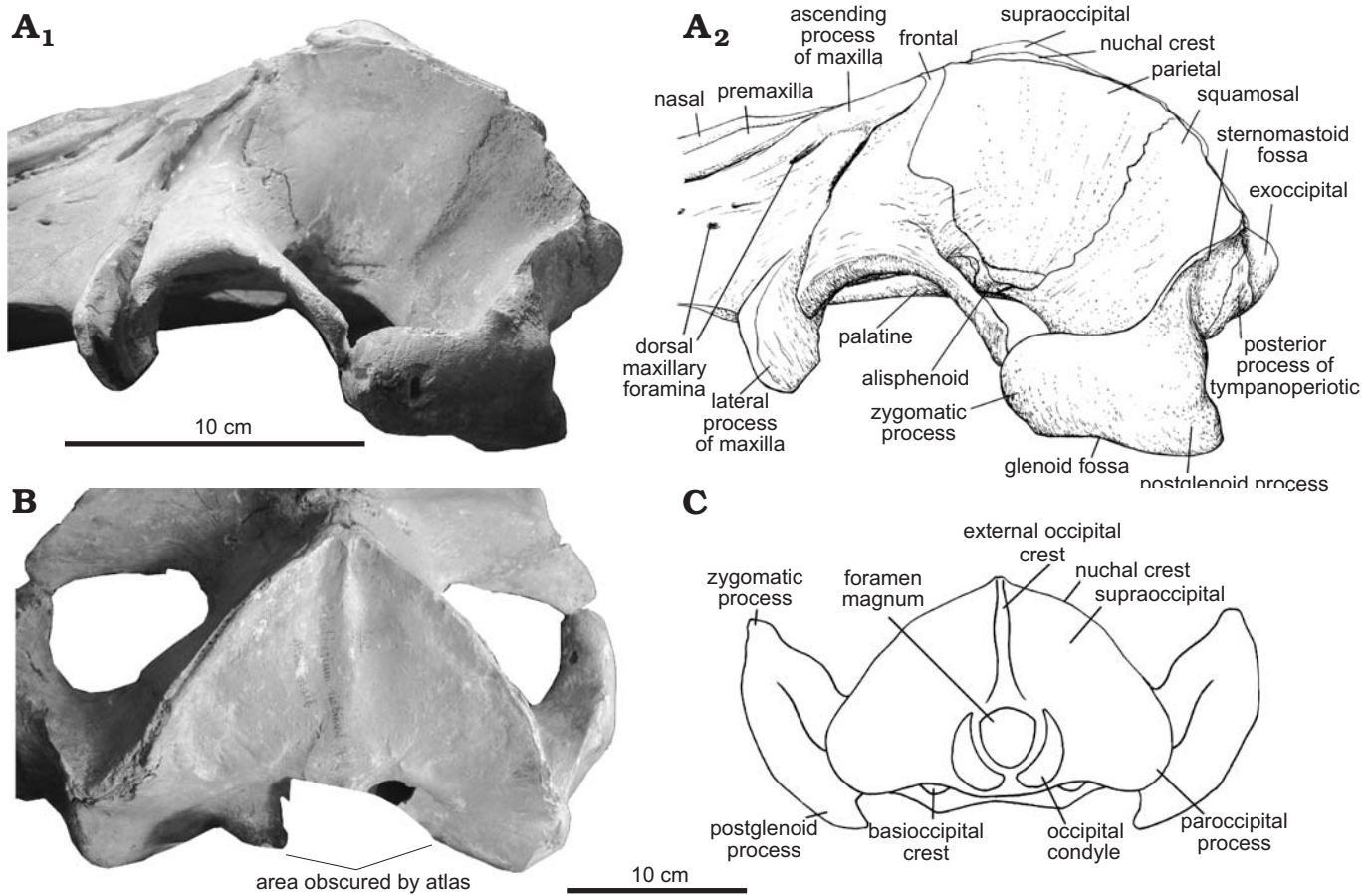


Fig. 7. Neurocranium of the cetotheriid baleen whale *Cetotherium riabinini* Hofstein, 1948, Late Miocene of Nikolaev, Ukraine, NMNH-P 668/1, in lateral (A), posterodorsal (B), and posterior (C) views. Photographs (A<sub>1</sub>, B), explanatory drawings (A<sub>2</sub>, C).

**Palatine.**—In ventral view, the palatine extends anteriorly beyond the level of the antorbital notch, and posteriorly to the level of the foramen pseudovale (Fig. 6B). The lateral margins of both palatines are damaged, but a transverse constriction in the posterior third of the left bone suggests a dumbbell shape as in *Cetotherium rathkii*. Together, the anterior margins of both palatines form a V-shaped, posteriorly pointing notch (Figs. 4D, 6B).

**Pterygoid.**—The anteroposteriorly elongate and transversely narrow medial lamina of the pterygoid borders the vomer medially, and the basioccipital crest posteriorly (Fig. 6B). The lateral lamina is irregularly shaped, approximating the lateral surface of the alisphenoid anterolaterally (Fig. 8) and the foramen pseudovale posterolaterally. The anteromedial margin of the lateral lamina is covered by the palatine (Fig. 6B). The pterygoid sinus fossa extends anteriorly to the level of the foramen pseudovale and is filled with matrix, thus obscuring the dorsal lamina of the pterygoid. The apex of the pterygoid hamulus is broken.

**Vomer.**—In ventral view, the vomer extends posteriorly to the anterior margin of the basioccipital crest and covers the basisphenoid-basioccipital suture. The posterior portion of the vomerine crest is low. Anteriorly, the vomer is poorly

preserved, but seems to have been clearly exposed on the ventral surface of the rostrum.

**Alisphenoid.**—The alisphenoid is largely covered by the pterygoid and squamosal. As a result, only its lateral portion is exposed in the temporal fossa, where it borders the parietal, frontal, pterygoid and squamosal (Fig. 8).

**Orbitosphenoid.**—In ventral view, the orbitosphenoid occurs as a large, triangular element anterior to the facial canal (Fig. 6B).

**Squamosal.**—In dorsal view, the supramastoid crest is sigmoidal and joins the nuchal crest at a right angle. The zygomatic process is not aligned with the lateral border of the exoccipital and instead clearly separated from the latter by a distinct angle (Fig. 6A). The zygomatic process is directed somewhat anterolaterally, short anteroposteriorly, wide transversely, and uniformly high dorsoventrally, which makes it extremely robust compared to that of other cetotheriids. In lateral view, a clearly developed sternomastoid fossa (Bouetel and Muizon 2006) is present between the supramastoid crest dorsally and the posterior process of the periotic ventrally. Ventrally, the squamosal bears a shallow, anteroventrally facing glenoid fossa. The foramen pseudovale is almost entirely enclosed by the squamosal, and medially bordered by the slender, irregularly shaped falciform process

(Fig. 6B). The postglenoid process is anteroposteriorly flattened, wide transversely, and slightly twisted medially (Figs. 4C, 6B). In lateral view, it projects posteroventrally, with a concave dorsal and a convex ventral border (Figs. 4B, 5C). The posterior portion of the postglenoid process is bent posterodorsally and directed medially.

**Exoccipital.**—The exoccipital forms a pentagonal plate, and is anteroposteriorly thickened where it forms the paroccipital process (Figs. 6B, 7A). A low, undulating crest extends horizontally from the dorsal margin of the foramen magnum. Ventral to the latter, a shallow fossa surrounds the occipital condyle, which thus appears to form a neck. The large paroccipital process is made of rugose bone, teardrop-shaped in lateral view, and extends posteriorly beyond the level of the occipital condyle to form the posteriormost point of the skull. In dorsal view, the supramastoid and nuchal crests do not extend on to the paroccipital process (Fig. 6A).

**Supraoccipital.**—In dorsal view, the supraoccipital bone is sub-triangular (Figs. 6A, 7B, C) and extends anteriorly to the level of the temporal fossa, but not beyond the apex of the zygomatic process. There are no distinct tubercles. Near the skull vertex, the nuchal and external occipital crests join together to form an elevated area. The nuchal crest is elevated above the occipital shield along almost its entire length and slightly convex in dorsal view. The external occipital crest is high along its anterior portion (Fig. 7B, C) and then becomes lower and transversely wider, before terminating in a wide, flat area dorsal to the foramen magnum.

**Basioccipital.**—The basioccipital is trapezoidal and partially covered by the posterior portion of the vomer (Fig. 6B). Laterally, the basioccipital contributes to the border of the cranial hiatus. The basioccipital crest is large and bulbous, with a flattened ventral surface. A low median crest represents the posterior extension of the vomerine crest.

**Periotic.**—Both bones are unprepared and covered by matrix or the underlying tympanic bulla. The composite posterior process of the periotic and tympanic bulla is relatively short and bears a deep (but not tube-like) facial sulcus. The distal surface of the posterior process is clearly exposed on the lateral skull wall as a subtriangular, dorsally directed wedge, interposed between the exoccipital and the squamosal (Figs. 3, 7A).

**Tympanic bulla** (Fig. 9).—The description is based on the right bulla as preserved in situ. The longitudinal axis of the bulla is oriented slightly anteromedially. In ventrolateral view, the tympanic bulla is oval or slightly kidney-shaped, whereas in ventral view the bone shows a markedly angular anteromedial corner and slightly narrows along its posterior third. The anterolateral portion of the ventral surface of the bulla is transversely concave. The sigmoid process is straight, moderately long, relatively massive, evenly thickened anteroposteriorly along its entire length, and directed slightly posteriorly (Fig. 9B, C). The base of the sigmoid process is located posterior to the centre of the bulla and not inflated, with the bone surface surrounding it being relatively smooth. In lateral view, the

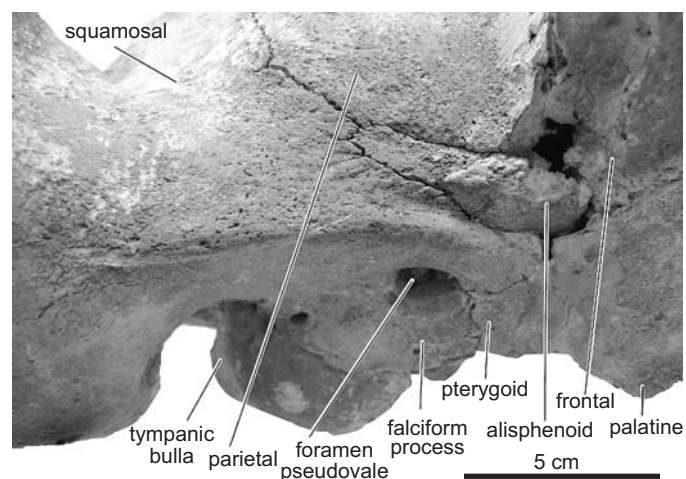


Fig. 8. Alisphenoid and adjoining bones of the cetotheriid baleen whale *Cetotherium riabinini* Hofstein, 1948, Late Miocene of Nikolaev, Ukraine, NMNH-P 668/1, in anterolateral and slightly ventral view.

bulla is oval in outline. In medial view, there is a distinct but low medial lobe, which is separated from its lateral counterpart by a subtriangular median furrow (Fig. 9D–F). The lateral lobe extends somewhat further posteriorly than the medial one. The main and involucral ridges converge anteriorly.

**Mandible.**—The distal portion of the mandible is straight (i.e., not bowed laterally) (Fig. 5). The condyle is large, elevated above the mandibular body, and increases in width dorsally (Fig. 10A, C). The dorsolateral portion of the condyle is twisted at an angle of  $45^\circ$  relative to the anteroposterior axis of the mandible (Fig. 10C). The angular process is massive, bulbous and somewhat extended posteriorly (Fig. 10A). Dorsal to the angular process, there is a notch for the internal pterygoid muscle located medial to the subcondylar furrow (Fig. 10B). The coronoid process is long anteroposteriorly, low dorsoventrally, and bent laterally. The postcoronoid crest is low. The mandibular foramen is dorsoventrally narrow and has a notched anterior margin. Damage to the bone has exposed part of the narrow mandibular canal (less than 10 mm in diameter anterior to the base of the coronoid process). An alveolar groove is present along the dorsomedial surface of the mandible and well developed near its distal end. The mandibular symphysis is unfused and marked by a 25 cm long symphyseal groove. The latter initially runs parallel to the anterior edge of the mandibular body, then turns  $90^\circ$  and continues posteriorly parallel to the lower edge of the body. In lateral view, the mandibular body is perforated by a series of mental foramina aligned in a single, longitudinal row.

In cross section, the outline of the mandibular body significantly changes anteroposteriorly (Fig. 11). The body is high, laterally flattened and symmetrical in the symphyseal area. Further posteriorly, it lowers and widens, and the dorsal crest flattens. Forty centimetres from the tip, the bone acquires an asymmetrical profile with a convex lateral surface and a flat medial one. The lower edge is convex and lacks a ventral crest. From this point onwards, the depth of the man-

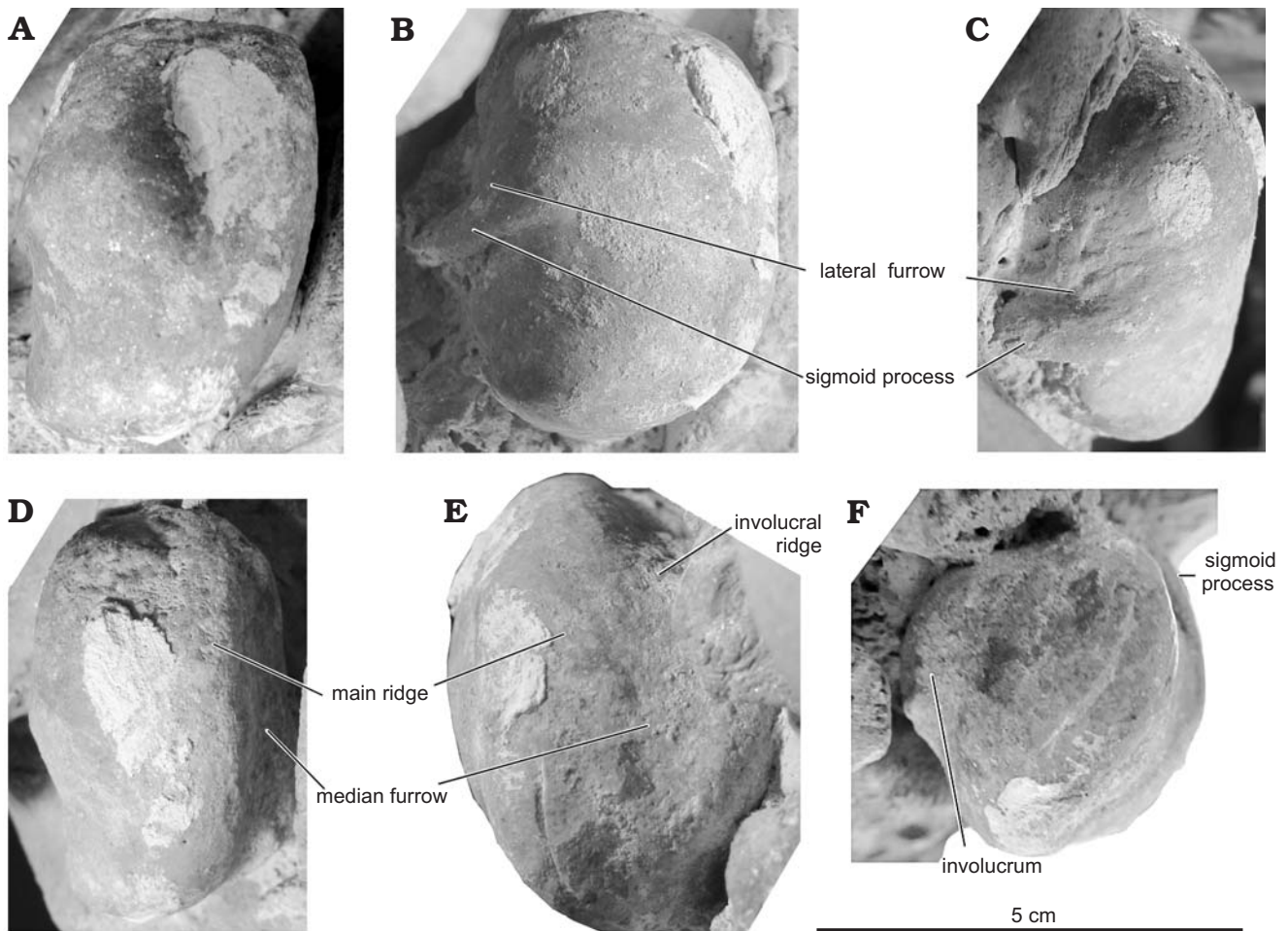


Fig. 9. Right tympanic bulla of the cetotheriid baleen whale *Cetotherium riabinini* Hofstein, 1948, Late Miocene of Nikolaev, Ukraine, NMNH-P 668/1, in ventral (A), ventrolateral (B), anterolateral (C), ventromedial (D), medial (E), and posterior (F) views.

dible gradually increases posteriorly. Seventy centimetres from the tip, the dorsal crest becomes sharp, and at 80 cm the mandible again becomes symmetrical, with rounded medial and lateral sides. Posterior to the coronoid process, the height of the mandible lowers, before rising again and reaching its maximum at the level of the condyle.

Measurements of the left and right mandibles reveal an obvious degree of asymmetry (Table 2), with the body of the left mandible being longer, more curved and slightly lower along its entire length. In addition, the proximal portion of the left mandible is longer, as is the base of its coronoid process (by 10 mm). There are no traces of either pathological or diagenetic deformation.

#### Vertebral column

Four cervical, 10 thoracic, 8 lumbar and 19 caudal vertebrae have been preserved (Figs. 12–14, Table 3), leading us to a total estimate of 46 or 47 (C7, T12, L8, Ca19–Ca20). Except for the cervicals, all of the vertebrae and their associated ribs show well-developed pachyosteosclerosis (see also Hofstein 1948). The epiphyses of C7 and all of the thoracic, lumbar and anterior caudal vertebrae are unfused. In Ca12–Ca17, the

epiphyses are fused, with the anterior suture having become partially obliterated in Ca12.

*Cervical vertebrae.*—C4–C7 are separate, with no signs of intervertebral fusion. The centra are subrectangular in outline and bear wide, slightly curved neural arches with low neural spines. Posterior to C4, the transverse processes are oriented anterolaterally. In C4, the symmetrical diapophysis and parapophysis connect laterally to form a transverse foramen. In C5, only the bases of the transverse processes have been preserved. In C6, the diapophysis is thickened and oriented ventrally, whereas the equally thickened parapophysis is short and oriented laterally. In C7, only the thick and transversely wide diapophysis is present. The prezygapophyses are generally small and the postzygapophyses underdeveloped, which is relatively unusual among mysticetes and may be a result of individual age variation.

*Thoracic vertebrae.*—Judging from available descriptions of *Piscobalaena nana* (Bouetel and Muizon 2006) and “*Cetotherium*” aff. *mayeri* (Spassky 1954), the thoracic vertebrae appear to have been mounted out of order (Figs. 13A, 15). Five complete vertebrae form part of the mounted skeleton, with the fragmented remains of a further 5 having been recon-

Table 2. Measurements (in mm) of the mandible of *Cetotherium riabinini*.

Measurement	Left	Right
Total length, measured in a straight line	920	935
Total length, measured along the lateral margin	970	945
Height at the coronoid process	68	71
Length from the posterior end of the coronoid process to the condyle	44	46
Length of the base of the coronoid process	102	92
Height of the coronoid process	52	48+
Height at the condyle and angular process	86	84+
Height at the distal end	40	40
Height at 10 cm from the distal end	50	50
Height at 20 cm from the distal end	39	46
Height at 30 cm from the distal end	42	45
Height at 40 cm from the distal end	45	48
Height at 50 cm from the distal end	50	49
Height at 60 cm from the distal end	53	56
Height at 70 cm from the distal end	55	56
Maximum width	46.5	48

Table 3. Measurements (in mm) of the vertebrae of *Cetotherium riabinini*.

Vertebra	Centrum length	Centrum width	Centrum height	Total height	Combined width across transverse processes
C4	8	54	40		125
C5	8	50	45		79+
C6	8	46			125
C7	10	49	48	87	119
TB	26	56	48	113.5	109
TC	31	58	45	124	105
TD	45	70	44	131	121
TE	31	62	42	119	136
TF	39	72	48	124	169
L1	40	69	48	129	204
L2	42.5	66	48	137	204
L3	42.5	68	50	153	212
L4	44	73	51	150	215
L5	44	74	48	135	209
L6	50	83	55	135	206
L7	50.5	78	60	137	200
L8	56	78	57	138	198
Ca1	58	81	61	139	180
Ca2	55	78	63	—	169
Ca3	58	77	63	—	153
Ca4	58	72	63	127	138
Ca5	56	69	64	113	110
Ca6	57	68	71	104	91
Ca7	60	60	68	92	75
Ca8	55	54	63	79	62
Ca9	55	48	56	69	53
Ca10	48	45	53	61	—
Ca11	39	43	46	52	—
Ca12	29	41	43	43	—
Ca13	24	41	31	—	—
Ca14	24	36	29	—	—
Ca15	24	35	23	—	—
Ca16	20	29	23	—	—
Ca17	18	24	18	—	—

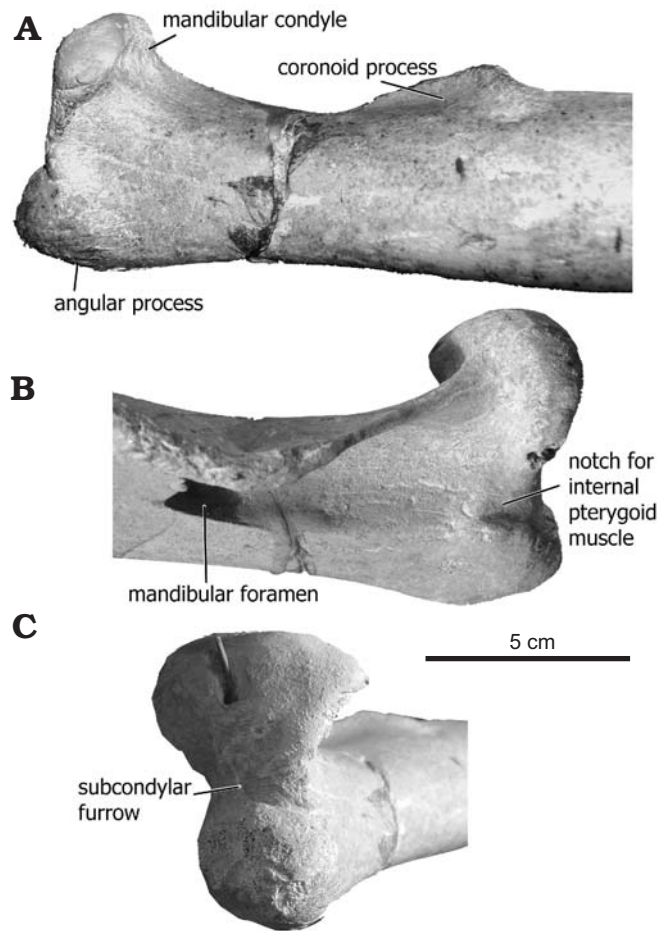


Fig. 10. Proximal portion of the right mandible of the cetotheriid baleen whale *Cetotherium riabinini* Hofstein, 1948, Late Miocene of Nikolaev, Ukraine, NMNH-P 668/1, in lateral (A), dorsomedial (B), and posterior (C) views.

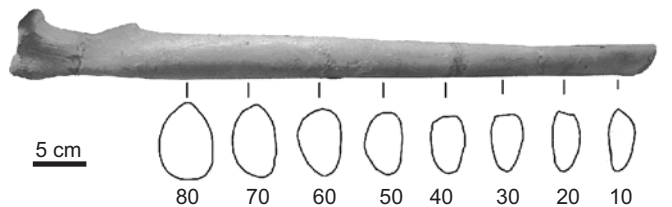


Fig. 11. Cross sections of the right mandible of the cetotheriid baleen whale *Cetotherium riabinini* Hofstein, 1948, Late Miocene of Nikolaev, Ukraine, NMNH-P 668/1, located 10–80 cm posterior to the distal end of the bone. For each cross section, the medial margin of the mandible is on the right.

structed using plaster. The anteriormost two vertebrae appear to be missing. Facets on the centra for the articulation with the rib capitula are present on the first three of the preserved vertebrae (TA–TC), here interpreted as T3, T4 or 5, and T7 or 8, respectively (Fig. 15). A small metapophysis occurs on the anterior margin of the transverse process of TA. On the subsequent vertebrae, the metapophyses increase in size and migrate medially, approaching the base of the transverse process and, ultimately, the neural arch.

*Lumbar vertebrae.*—All lumbar vertebrae (8 in total) appear to have been preserved. The centra are oval in anterior

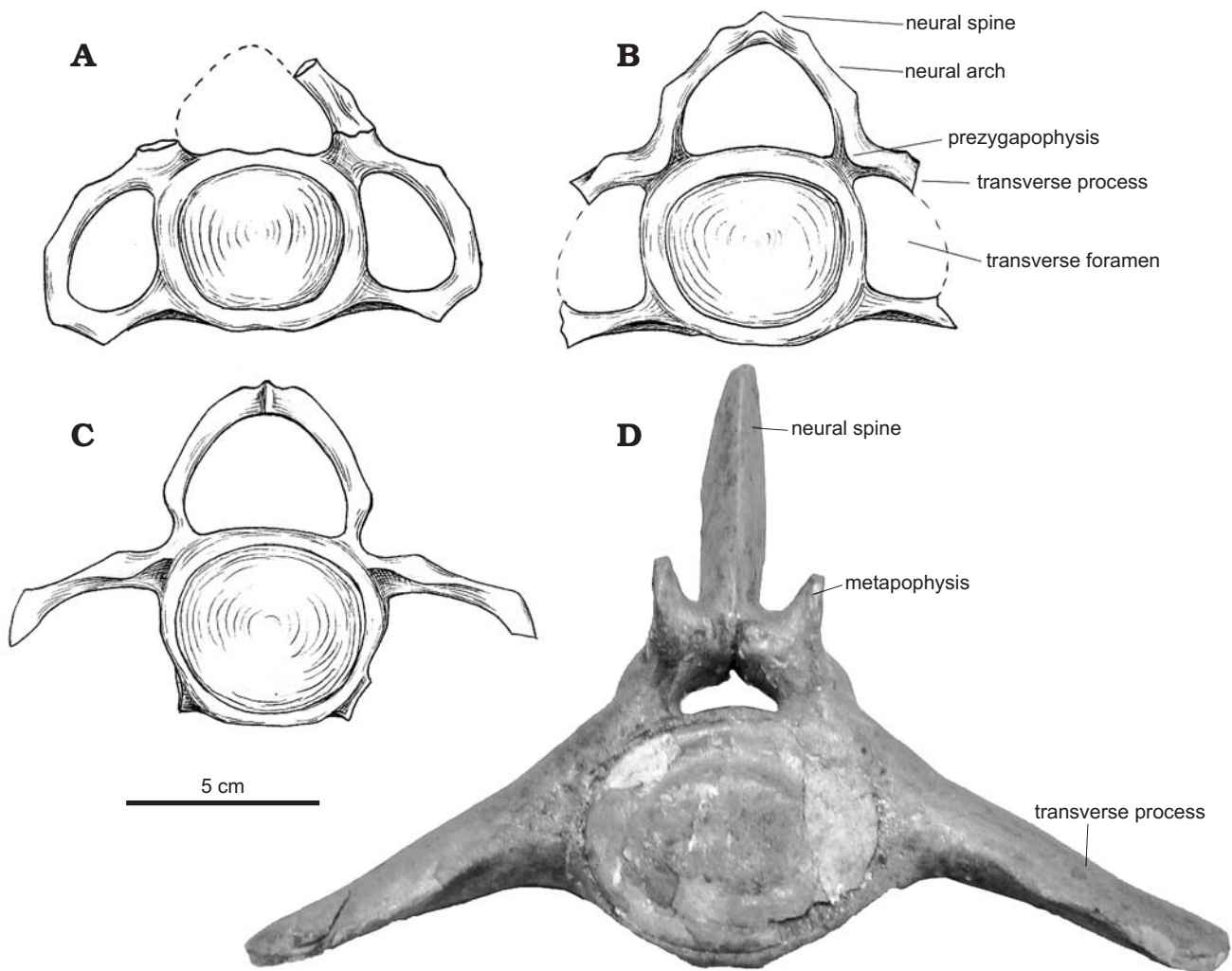


Fig. 12. Selected vertebrae of the cetotheriid baleen whale *Cetotherium riabinini* Hofstein, 1948, Late Miocene of Nikolaev, Ukraine, NMNH-P 668/1, in anterior views: C4 (A), C5 (B), C7 (C), L7 (D). Photograph (D), explanatory drawings (A–C).

view and flattened dorsoventrally, with height: width ratios of 0.65–0.76 (Table 3). L1–L3 are characterised by posteroventrally oriented, narrow (but long) transverse processes, high and posteriorly inclined spinal processes, and massive, laterally compressed metapophyses. In L4, the transverse process is oriented laterally, before becoming oriented anterolaterally from L5 onwards (Fig. 13A). In L1–L4, and especially L2–L3, the anterior margin of the spinal process is markedly concave (Fig. 13B). Posterior to L4, the spinal process develops a straight anterior edge and becomes wider anteroposteriorly, as well as more posteriorly inclined.

**Caudal vertebrae.**—19 caudal vertebrae have been preserved (Fig. 14). Ca1 differs from the posteriormost lumbar vertebra in having paired ventral processes for a chevron bone, as well as a shortened transverse process. The bases of the metapophyses converge anterior to the neural arch. Ca2 and Ca3 have a square transverse process, which is separated from the centrum by a deep groove in dorsal and anterior view (Fig. 13A); the same groove occurs posteriorly on Ca4. Unlike in most other mysticetes, including “*Cetotherium*” *mayeri*-like

whales from the Eastern Paratethys and *Piscobalaena nana*, there are no vertical foramina perforating the transverse process of any of the caudal vertebrae (Brandt 1873; Spassky 1954; Bouetel and Muizon 2006).

Along Ca4–Ca10, the metapophyses, neural arches, and spinal and transverse processes gradually reduce in size, with the latter completely disappearing posterior to Ca7. The centra narrow transversely along their posterior portions, giving them the shape of a flattened cone in dorsal view. In Ca11, the centrum shortens abruptly, thus losing its conical shape. The neural arch is absent, and the metapophysis is small. From Ca12 onwards, the vertebrae are roughly spherical and irregular in shape. From Ca13 onwards, the vertebrae are divided into an anterior and a posterior half by a transverse groove. Posterior to Ca13, the spinal process completely disappears (Fig. 14). Although the posteriormost caudal vertebrae are often missing, the presence of 7 shortened posterior vertebrae with no obvious processes, which in living mysticetes correspond to the fluke region, implies that the vertebral column of *Cetotherium riabinini* is essentially complete.

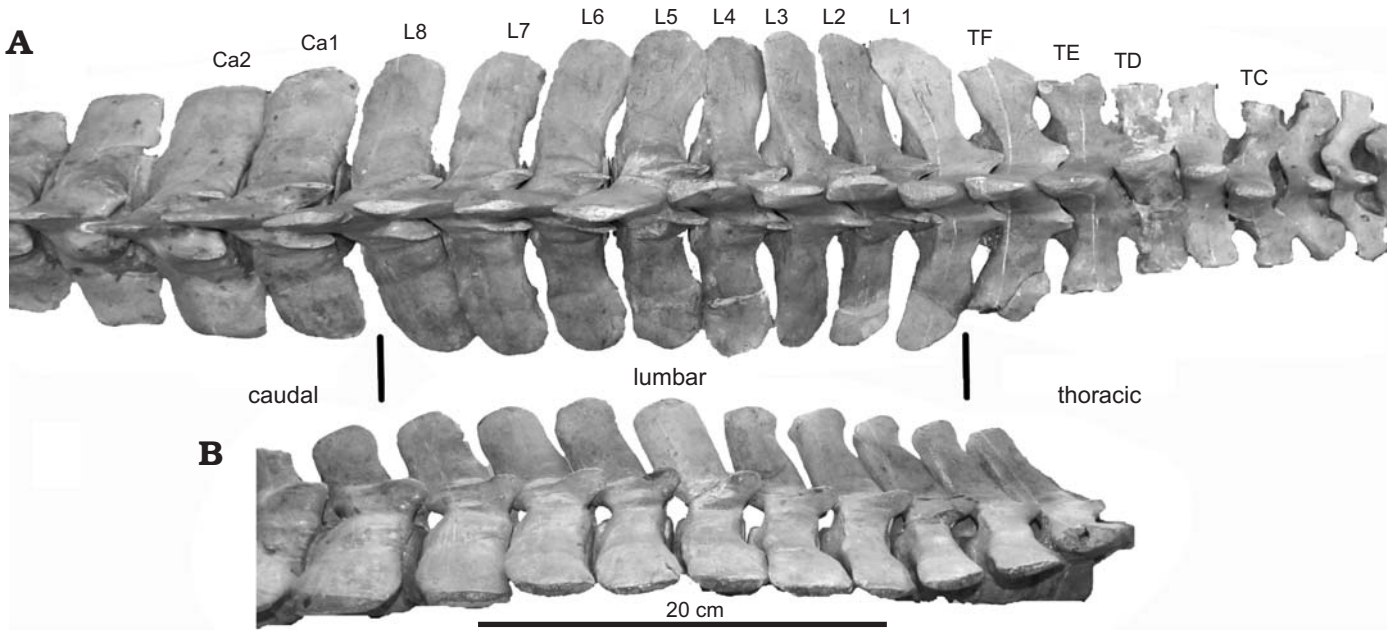


Fig. 13. Vertebrae forming part of the torso (sensu Buchholtz 2001) of the cetotheriid baleen whale *Cetotherium riabinini* Hofstein, 1948, Late Miocene of Nikolaev, Ukraine, NMNH-P 668/1, in dorsal (A) and lateral (B) views.

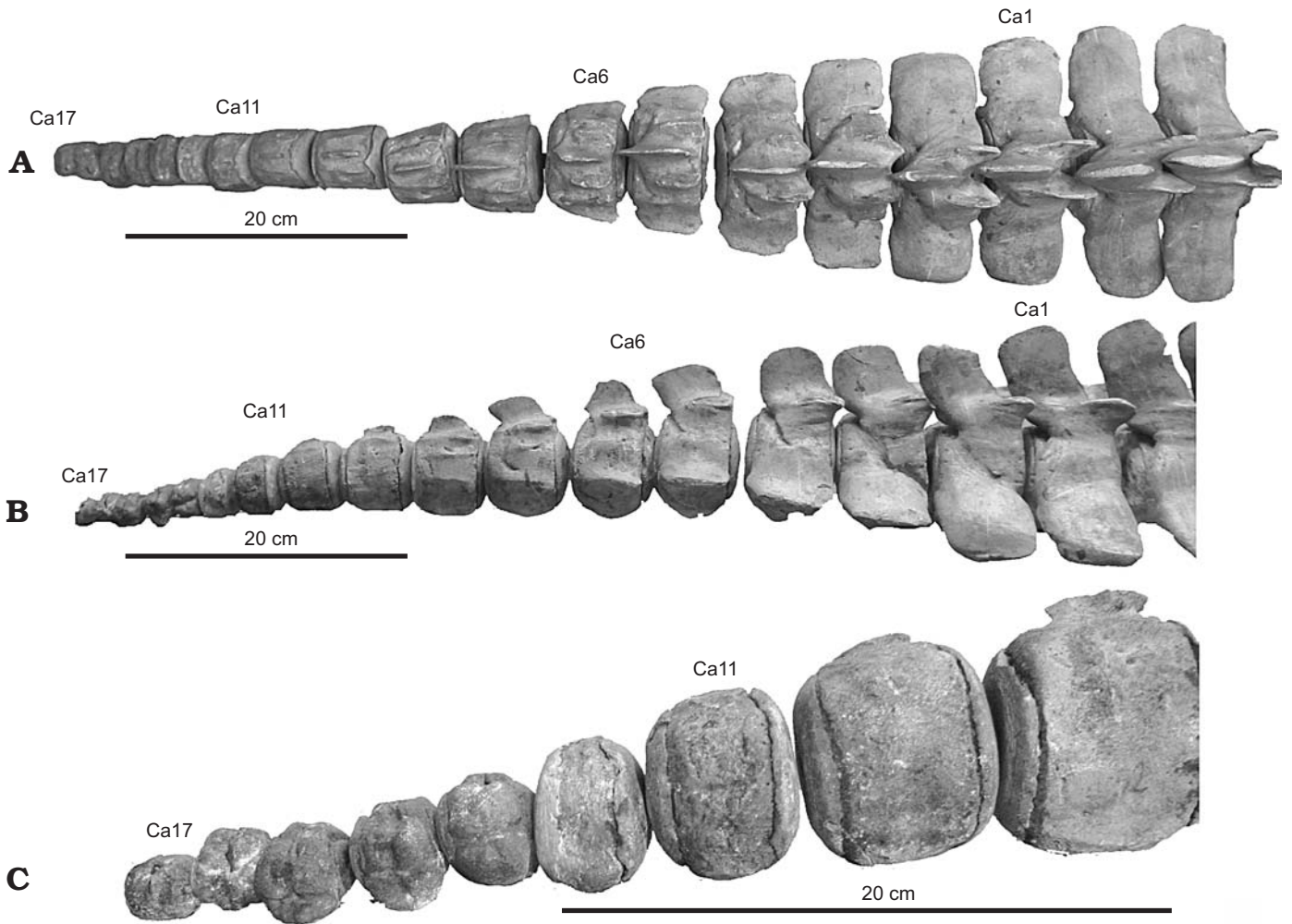


Fig. 14. Caudal vertebrae of the cetotheriid baleen whale *Cetotherium riabinini* Hofstein, 1948, Late Miocene of Nikolaev, Ukraine, NMNH-P 668/1, in dorsal (A) and lateral (B, C) views.

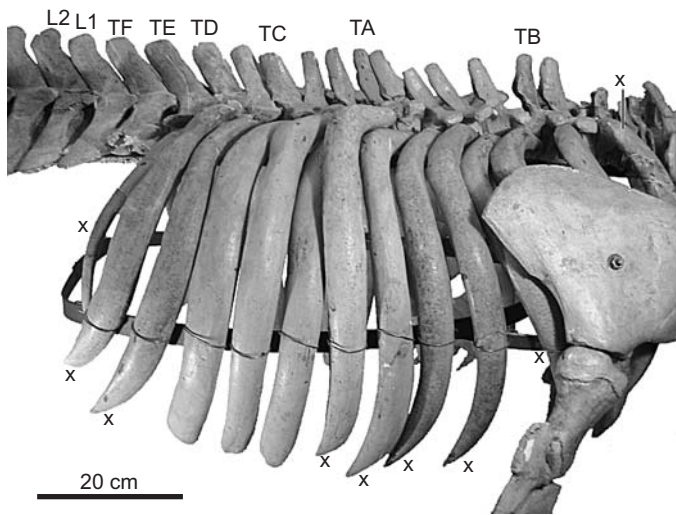


Fig. 15. Ribs of the cetotheriid baleen whale *Cetotherium riabinini* Hofstein, 1948, Late Miocene of Nikolaeiv, Ukraine, NMNH-P 668/1, in right lateral view; x denotes actually preserved (as opposed to remodelled) bones.

**Ribs.**—Hofstein (1948, 1965) reported that 11 pairs of ribs had been preserved, (it is unclear whether all of them were present on both sides), with 9 of them being complete. Many of the ribs are fragmentary and re-modelled, making it difficult to describe them accurately. However, there are at least 8 to 9 right ribs and 3 left ribs present in the mounted skeleton. The first one or two pairs are absent, which corresponds to the absence of the first two thoracic vertebrae. Almost all of the ribs are extensively thickened. The anteriormost rib is shortened and curved, and followed by a series of sickle-shaped anterior ribs with well-developed capitula and small tubercula. The central ribs are sigmoidal in lateral view (“spiral” according to Hofstein 1948) (Fig. 15). The capitula are absent on the three posteriormost ribs (two according to Hofstein 1948, 1965). The last rib is sickle-shaped, and shorter and thinner than any of the others. None of the preserved ribs show any evidence of articulation with the sternum.

#### Forelimb

**Scapula.**—The scapula is roughly triangular, fan-shaped, and relatively short anteroposteriorly (Fig. 16, Table 4). The anterior margin is blunt and rounded, while the posterior margin is elongated. The robust acromion is rounded anteriorly and forms a sharp angle with the anterior margin of the scapular blade. The coracoid process is robust, but short, and slightly curves towards the acromion. The spine is reduced, flattened and shifted anteriorly. The portion of the scapula bearing the glenoid cavity is slightly concave medially. A low ridge bordering the infraspinous fossa posteriorly is developed on the lateral surface of the posteriormost portion of the scapular blade, and in particular near the glenoid cavity.

**Humerus.**—The humerus is flattened and dumbbell-shaped in lateral view (Fig. 16, Table 4). The posterior edge of the shaft is shorter than the anterior one as a result of the extensive development of the ulnar facet at the distal epiphysis. Both the greater and lesser tubercles are well developed, and

divided by a shallow furrow. Only the distal epiphysis of the left humerus is fused to the shaft.

**Radius.**—The radius is transversely flattened and slightly curved anteriorly in lateral view (Fig. 16, Table 4). Both of the distal epiphyses are fused, unlike their proximal counterparts.

**Ulna.**—The ulna is transversely flattened and sigmoidal in lateral view. The olecranon is well developed and proximally elongated (Fig. 16, Table 4). Only the distal epiphyses are fused to the shaft.

**Carpus, metacarpus, and phalanges.**—According to Hofstein (1965), the carpals, metacarpals and most of phalanges have not been preserved. In the mounted skeleton, it is difficult to distinguish genuine bones from those remodelled for display. As far as can be told, the metacarpals and proximal phalanges are dumbbell-shaped, while the distal phalanges are elongated and conical.

**Pelvis and hindlimb.**—According to Hofstein (1948, 1965), both of the pelvic bones and femora were found with the skeleton. Unfortunately, both elements are currently missing. As noticed by Hofstein (1965: 26), the pelvic bones were elongated, while the femora “looked like oval plates”, with a diameter of up to 5 cm.

**Remarks.**—Unlike the adult holotype of *Cetotherium rathkii*, that of *C. riabinini* represents a juvenile or sub-adult. Nevertheless, we consider it unlikely that the morphological differences between them are simply the result of ontogenetic variation. In living baleen whales, the orientation of the squamosal generally does not change during ontogeny (PG, personal observation). By contrast, the zygomatic process can expand during growth—at least in living odontocetes. In this light, the ontogenetically young *C. riabinini* seems more anatomically “adult” (peramorphic) than *C. rathkii*, with differences in the morphology of the squamosal (and, possibly, the facial region) likely reflecting the specific anatomy of the jaw attachment.

“*Cetotherium*” *klinderi*, another Neogene fossil mysticete known from the Black Sea region, was mainly defined based on the distinctive anatomy of a tympanic bulla from Chişinău

Table 4. Measurements (in mm) of the forelimb of *Cetotherium riabinini*.

Length of scapula	148
Height of scapula	212
Length of humerus	122
Proximal width of humerus	68
Minimum width of humerus	47
Distal width of humerus	61
Length of anterior margin of radius	175
Length of posterior margin of radius	138
Proximal width of radius	38
Distal width of radius	42
Length of anterior margin of ulna	149
Length of posterior margin of ulna	176
Proximal width of ulna	38
Distal width of ulna	48
Length of olecranon	52

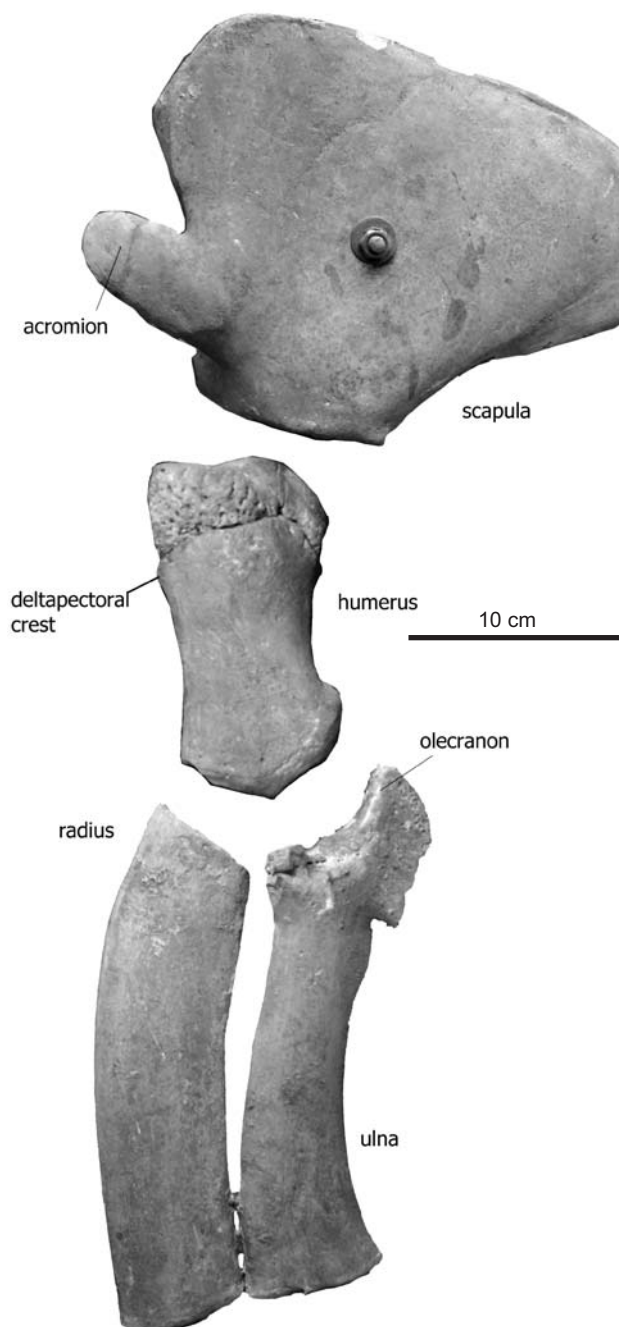


Fig. 16. Left forelimb of the cetotheriid baleen whale *Cetotherium riabinini* Hofstein, 1948, Late Miocene of Nikolaev, Ukraine, NMNH-P 668/1, in lateral view.

(Kishinev), Moldova. The latter clearly differs from that of other species of *Cetotherium* in having a widened posterior portion in medial view, as well as a strongly inflated involucrum (Brandt 1873: pl. 12: 4). “*C.*” *klinderi* can thus be excluded as a potential senior synonym of *C. riabinini*. Note that a second specimen of “*C.*” *klinderi* from Nikolaev reported by Brandt (1873) is not available for study at present, and has possibly been lost.

*Geographic and stratigraphic range.*—Type locality and horizon only.

## Discussion

**Anatomy of the ribs and vertebral column.**—Pachyosteosclerosis of the vertebrae and ribs is an archaic cetacean trait found in archaeocetes and early mysticetes (Buffrénil et al. 1990; Gray et al. 2007). One of the youngest occurrences of cetacean pachyosteosclerosis outside the Eastern Paratethys is represented by *Diorocetus hiatus* from the Middle Miocene (Beatty and Dooley 2009). Pachyosteosclerosis is less developed in cf. *Metopocetus* sp. VMNH 1782 (Beatty and Dooley 2009) of the same age, and completely absent in the Late Miocene *Piscobalaena nana* (Bouetel and Muizon 2006). By contrast, strong postcranial pachyosteosclerosis characterises all of the Late Miocene whales from the Eastern Paratethys, including *Cetotherium priscum*, “*Cetotherium*” *klinderi*, *Eucetotherium helmersenii*, “*Cetotherium*” *mayeri*, and “*Cetotherium*” aff. *mayeri* (Brandt 1873; Hofstein 1948; Spassky 1954). The living *Caperea marginata* also has pachyostotic, but not osteosclerotic ribs. Nevertheless, *Cetotherium riabinini* and *Caperea marginata* are at least superficially similar in having wide, sigmoidal ribs which partially overlap to form a solid lateral wall of the rib cage (Bisconti 2012).

The vertebrae of *Cetotherium riabinini* are relatively small compared with those of other Neogene mysticetes, including cetotheriids such as *Piscobalaena nana* and “*Cetotherium*” aff. *mayeri* (Bouetel and Muizon 2006; Spassky 1954). In terms of their shape, the cervical vertebrae of *C. riabinini* resemble those of *P. nana* (Bouetel and Muizon 2006), while the thoracic and lumbar vertebrae are similar to those of both *P. nana* and “*Cetotherium*” *mayeri* (Brandt 1873). The posteriormost (12<sup>th</sup>) thoracic vertebra of *C. riabinini* is most similar to the 10<sup>th</sup> vertebra of *P. nana* (Bouetel and Muizon 2006: fig. 21). The number of lumbar vertebrae of *Cetotherium riabinini* is the smallest of any mysticete except *Caperea marginata* (Buchholtz 2011). Similarly, the total number of caudal vertebrae appears to be unusually low (but similar to living *Caperea marginata* and *Balaenoptera acutorostrata*), whereas the number of thoracic vertebrae resembles that of other mysticetes (True 1904; Buchholtz 2007, 2011). This may indicate parallel meristic reduction of the lumbar and caudal series, implying neocete modularity (Buchholtz 2007, 2011).

While the small number of elongated lumbar and anterior caudal vertebrae of *Cetotherium riabinini* may point to a relatively flexible torso (sensu Buchholtz 2001), the lack of vascular foramina in the caudals may correlate with a stiff tail. The latter likely bore large flukes, as indicated by the relatively long distal portion of the caudal series. The heavy pachyosteosclerotic skeleton likely resulted in a relatively low degree of overall manoeuvrability, especially given the relatively small body size. Taken together, the postcranial skeleton of *C. riabinini* thus considerably differs from that of most other mysticetes, and may instead be functionally analogous to that of sirenians (Buffrénil et al. 2010).

**Phylogeny.**—Our phylogenetic analysis resulted in 9 most parsimonious trees of 386 steps (CI = 0.55, RI = 0.85) (Fig. 17), and confirms the monophyly of both the genus *Cetotherium* (comprising *C. rathkii* and *C. riabinini*) and Cetotheriidae as a whole, with *Mixocetus elysius* and *Joumocetus shimizui* as its basalmost members. While both species of *Cetotherium* share an anteriorly widened tympanic bulla, Cetotheriidae are united by (i) an anterolaterally oriented antorbital process of the maxilla; (ii) a posteriorly shifted premaxilla, maxilla and parietal; and (iii) an expanded distal surface of the compound posterior process of the tympanoperiotic (see also Marx 2011). Considering *Herpetocetus* spp. to be the most derived and *J. shimizui* and *M. elysius* as the basalmost cetotheriids, we conclude that *Cetotherium* combines both primitive and derived traits, with a predominance of primitive characteristics. Primitive traits include the morphology of the exoccipital and the posterior portion of the maxilla, as well as the transversely oriented postglenoid process. By contrast, the narrow rostrum, the transversely compressed lateral portion of the squamosal, and the triangular occipital shield bearing a low external occipital crest likely represent derived features.

Previous cladistic studies (Bouetel and Muizon 2006; Steeman 2007; Bisconti 2008, 2012; Marx 2011, Fordyce and Marx 2012) have disagreed on the detailed interrelationship of cetotheres. Our study adds to a considerable number of described cetotheres ranging from the late Middle Miocene to the Pliocene, with some of the oldest confirmed cetotheriids known from the middle Sarmatian (late Middle Miocene; Neveeskaya et al. 2003) of the Eastern Paratethys (e.g., Brandt 1873; Kellogg 1929; Riabinin 1934; Spassky 1954; Mchedlidze 1964; Bouetel and Muizon 2006; Whitmore and Barnes 2008; Boessenecker 2011). These records show that a taxonomically diverse Northern Hemisphere cetother fauna already existed during the Tortonian and possibly even Serravallian, thus likely placing the initial diversification of cetotheres into or prior to the early Middle Miocene (see also Fordyce and Marx 2012). There are currently no described cetother-like taxa from this period, and we expect that settling the question of cetother interrelationships will likely have to await the discovery of these earliest members of the family.

**Feeding strategy.**—While some previous studies suggested a similar feeding strategy for cetotheriids and balaenopterids (e.g., Bouetel 2005), most interpreted cetotheres to have followed a more unique path (Kimura 2002, 2005, 2006, 2008, 2012; El Adli and Boessenecker 2011). Living balaenopterids feed by engulfing vast quantities of water and prey using an expanded oral cavity (throat pouch). This process involves rotation of the considerably curved mandibles around three separate axes, as well as fixation of the closed lower jaw by means of a cam articulation between the coronoid process of the mandible and the infraorbital plate of the maxilla (Carte and Macalister 1868; Beaugard 1882; Schulte 1916; Lambertsen 1983; Lambertsen et al. 1995; Lambertsen and Hintz 2004; Arnold et al. 2005).

Although superficially similar to balaenopterids in hav-

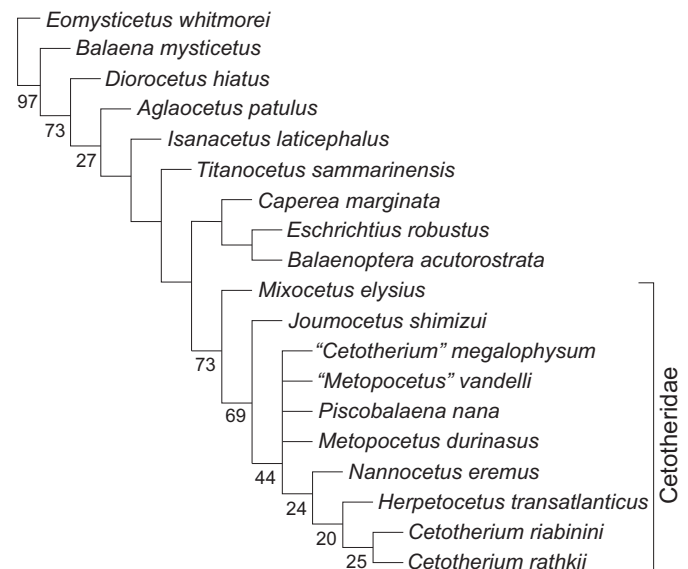


Fig. 17. Strict consensus of the 9 most parsimonious trees (386 steps, CI = 0.55, RI = 0.85) arising from the phylogenetic analysis. Numbers below branches indicate bootstrap support values.

ing both a laterally curved coronoid process and rostral bones interdigitating with the frontals, the following features likely prevented *Cetotherium riabinini* from rorqual-like gulp feeding: (i) the narrow rostrum, as well as the straight distal portion and rounded ventral crest of the mandible, indicate that the oral cavity was narrow and the throat pouch either small or altogether absent (Pivorunas 1977; Kimura 2002); (ii) the posterodorsal orientation of the mandibular condyle and the shallow glenoid fossa of the squamosal limit the possible degree of rotation of the mandibles, and restrict the opening of the mouth; and (iii) the low coronoid process suggests that the cam articulation of the mandible with the maxilla was either absent or less effective than in balaenopterids.

Many of the features seemingly preventing cetotheres from gulp feeding make them similar to suction-feeding cetaceans, in particular the grey whale *Eschrichtius robustus* (Lilljeborg, 1861) (Ray and Schevill 1974; Johnston and Berta 2011). However, suction feeding in the latter is associated with the presence of an arched rostrum and a well-developed pterygoid muscle, as suggested by the robust pterygoid hamuli (Johnston and Berta 2011). By contrast, the rostrum is straight and the hamuli gracile in *C. riabinini*, indicating that other suction-feeding animals may provide better models (Sanderson and Wassersug 1993). Filter-feeding ducks (Anatidae), such as the mallard *Anas platyrhynchos*, take in water and food with frequent, vertical movements of the lower jaw (Zweers 1974; Dawson et al. 2011). This process involves movement of the maxilla, quadrate, jugal, palatine and nasal, as well as the bending of the upper jaw at the naso-frontal hinge, owing to coupled kinesis of the skull bones (Bock 1964). Pendular movements of the quadrate, which itself is connected to the coronoid process, allow both the upper and lower jaws to move at a high rate. Thus, this feeding strategy requires continuous effort, unlike the inter-

mittent suction feeding employed by some teleost fishes and eschrichtiids (Sanderson and Wassersug 1993).

Previous studies remarked on the potentially analogous feeding strategies of cetotheres and anatids, pointing out the similarity of the well-developed, posteriorly extended angular process in cetotheres and the large retroangular process in ducks (Kimura 2002, 2006, 2008). We agree with this assessment, which we believe is further corroborated by the presence of a well-developed paroccipital process and a massive lateral process of the maxilla (the latter being functionally analogous to the lacrimal in the mallard) in *Cetotherium riabinini*. Specifically, the angular and paroccipital processes may have served as attachment sites for a well-developed m. depressor mandibulae, analogous to the digastric muscle of other mammals (Schulte 1916). The mandible, aided by its own weight to overcome water resistance, would first have been lowered by the action of the m. depressor mandibulae, and the lifted up again by the superficial masseter attached to the massive lateral process of the maxilla. An extreme example of such a feeding mode may be found in *Herpetocetus*, in which the mandible could probably only move in a vertical direction as a result of the transverse compression and rotation of the postglenoid process.

The comparison of cetotheres to filter-feeding ducks may also, at least in part, help to explain the occurrence of cranial kinesis in mysticetes (e.g., Deméré and Berta 2008). Similar to the kinetic arrangement of the skull bones in the mallard, the premaxilla, maxilla, lacrimal, jugal, and palatine of *Cetotherium riabinini* are only loosely connected both with each other and with the neurocranium, with the posteriorly shifted vomer potentially guiding their longitudinal movements. In addition, the posteriorly convergent ascending processes of the maxillae resemble the contacting maxillae and nasals of the mallard, and the jugal and lacrimal of mysticetes occupy positions similar to those of the quadrate and jugal of birds. However, *C. riabinini* markedly differs from the mallard in other aspects of its skull architecture, such as the structure of the mandibular condyle and its narrow rostrum (although it should be noted that the rostra of other cetotheriids are considerably wider). In addition, some anatine-like anatomical traits, such as a double coronoid process (Bisconti 2008) occur in eschrichtiids instead of cetotheres, thus implying that an anatine-like morphology may be indicative of both continuous and intermittent suction feeding strategies.

Other distinct anatomical traits of *C. riabinini* may also potentially be explained by its feeding strategy. Thus, the relatively small occipital shield for the attachment of the neck muscles (as opposed to balaenids, *Caperea* and, to some degree, balaenopterids, and eschrichtiids) indicates a reduced need to fix the head during feeding and, together with the enlarged basioccipital crests for the attachment of the well-developed m. longus capitis and m. rectus capitis anticus minor (Schulte 1916), suggests a relatively high level of neck flexibility. This conclusion is further supported by the presence of unfused cervical vertebrae bearing well-developed crests for the attachment of the neck musculature. In addition, the ros-

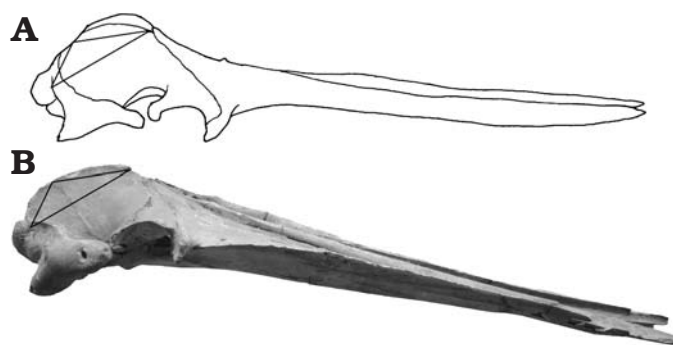


Fig. 18. Comparison of the lateral skull profile of the cetotheriid baleen whales *Piscobalaena nana* (redrawn from Bouetel and Muizon 2006, inverted) and *Cetotherium riabinini*. The images are aligned based on triangles connecting the exoccipital-petrotympenic-squamosal, squamosal-parietal-supraoccipital and supraoccipital-parietal (interparietal) sutures. Not to scale.

trum of *C. riabinini* is oriented somewhat ventrally (with no signs of pathological or diagenetic deformation), as becomes obvious when the skull is compared to that of *Piscobalaena nana* (Fig. 18). In small odontocetes following a benthic feeding strategy, such as *Sotalia* (Monteiro-Filho et al. 2002) and *Phocoena* (Galatius and Gol'din 2011; Galatius et al. 2011), a ventrally deflected rostrum may aid in the search for prey using echolocation, although it is possible that it may also be involved in suction feeding behaviour.

In the case of *C. riabinini*, feeding with a ventrally-pointing rostrum would likely have been ineffective. Equally, feeding with the rostrum lifted to a horizontal position might have been hindered by water resistance. It is thus possible that *C. riabinini* was feeding on its side, like lateralised feeding balaenopterids (Tershy and Wiley 1992) or suction-feeding grey whales (Ray and Schevill 1974; Woodward and Winn 2006). This may be reflected in the asymmetry of the mandibles and palatal nutrient foramina, and fits well with the presence of pachyosteosclerosis, which is commonly considered to be an adaptation for buoyancy control (Buffrénil et al. 1990; Gray et al. 2007) and benthic feeding (Beatty and Dooley 2009). Note that a similar, lateralised benthic feeding behaviour has also been suggested for *Diorocetus hiatus* (Beatty and Dooley 2009). This feeding strategy, combined with a slow-swimming lifestyle, could have been effective in areas with a high abundance of food. Interestingly, all published records of cetotheriids have been reported from areas of high primary productivity, including the Iberian Peninsula (Vandelli 1831), the North Sea (Van Beneden 1872), the East Coast of the United States (Cope 1896), California (Kellogg 1929; Whitmore and Barnes 2008), Peru (Bouetel and Muizon 2006) and Japan (Kimura and Hasegawa 2010). Similarly, the Eastern Paratethys of the Sarmatian age was highly productive (as are the present-day Sea of Azov and the northern Black Sea), as indicated by abundant biogenic sedimentation (Radionova et al. 2012).

Finally, some aspects of the morphology of *C. riabinini*, and indeed cetotheres as a whole, that might provide further

insights into feeding behaviour remain largely unknown. Most important among these are the morphology of the jugal and the hyoid bones. In both the mallard and suction-feeding cetaceans, the laryngeal musculature and the hyoid apparatus are well developed (MacLeod et al. 2007; Werth 2007), and in suction-feeding cetaceans the stylohyals are considerably curved (Johnston and Berta 2011). We thus hypothesise that future discoveries of complete sets of cetotheriid hyoid bones might reveal them to be both large and, possibly, of a relatively unusual shape.

## Conclusions

*C. riabinini* is a distinct species of *Cetotherium* known from a virtually complete skeleton from the early Tortonian of the Eastern Paratethys. The presence of a reduced number of lumbar and caudal vertebrae may indicate a parallel reduction in the length of two series, and thus neocete modularity. Similar to the living grey whale, *C. riabinini* was likely a lateralised, benthic suction feeder, and may have employed a feeding strategy analogous to the continuous suction feeding of the mallard—although the possibility of eschrichtiid-like intermittent suction feeding cannot be excluded. Convergent evolution driven by similar feeding strategies may partly explain the difficulties in reconstructing mysticete interrelationships above the family level, as many of the characters commonly used in phylogenetic analyses may have evolved independently several times. This factor should be taken into account in future phylogenetic studies.

## Note added in proofs

After the paper was accepted for the publication, an additional search revealed hitherto unavailable fragments at NMNH-P. Below, we provide a brief description (Fig. 19) and discussion.

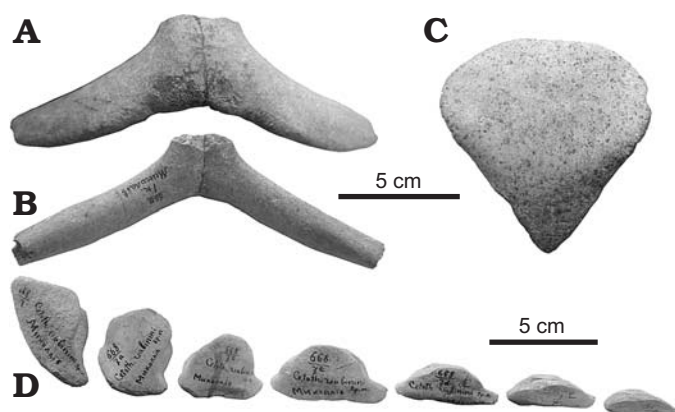


Fig. 19. Hyoid, sternum, and chevron bones of the cetotheriid baleen whale *Cetotherium riabinini* Hofstein, 1948, Late Miocene of Nikolaev, Ukraine, NMNH-P 668/1, hyoid in ventral (A) and anterodorsal (B) views, sternum in ventral view (C), chevron bones in left lateral view (D).

**Hyoid.**—Only the fused basihyal and thyrohyals are preserved. There is no sign of any suture between these elements. Except for a slight degree of pachyosteosclerosis, this hyoid resembles that of *Piscobalaena nana* (see Bouetel and Muizon 2006). The thyrohyals are robust, stick-like and oval in cross section. Their maximum width (span between posterior cornuas) is 127 mm. The anterodorsal cornuas are underdeveloped, implying that the ceratohyals may have been developed as separate bones (as in some odontocetes: see Reidenberg and Laitman 1994).

**Sternum.**—The sternum is a dorsoventrally flattened, heart-shaped bone showing bilateral asymmetry (the right side being wider), with a maximum width of 75 mm and a maximum height of 78 mm. The morphology of this bone is unique among cetaceans, differing from balaenopterids in lacking an elongate posterior process, and from balaenids in having a pointed, rather than blunt, posterior edge. The anatomy of the cetotheriid sternum is largely unknown, except for a specimen forming part of a postcranial skeleton from Nikolaev referable to *Cetotherium klinderi*. This specimen was originally described by Brandt (1871, 1873) and is now unavailable for study. However, its unusual shape seems to have been virtually identical to that of *C. riabinini*.

**Chevron bones.**—In total, we discovered seven bones, all of which vary markedly in shape depending on their original position: the anterior bones are high (resulting in a triangular outline in lateral view), whereas the posteriormost bones are low, but long.

## Acknowledgements

We thank Dmitry Ivanov (NMNH-P), Maria Rakhmanina and Valentina Stolbova (both National University of Mineral Resources “Mining University”, St. Petersburg, Russia), Konstantin Tarasenko (PIN), Gilles Cuny (University of Copenhagen, Copenhagen, Denmark), Vladimir Lobkov (ONU), and Gennady Baryshnikov (Zoological Institute, Russian Academy of Sciences, St. Petersburg, Russia) for their help and access to museum collections; Mette Steeman (Department of Natural History and Palaeontology, The Museum of Southern Jutland, Gram, Denmark) and Felix Marx (National Museum of Nature and Science, Tsukuba, Japan) for discussing cetacean anatomy and taxonomy, comments on an early draft of the manuscript, and for providing photographs of various Neogene mysticetes; Michelangelo Bisconti (San Diego Natural History Museum, San Diego, USA) for providing data on *Titanocetus sammarinensis*; Natalia Kryukova (Russian Federal Research Institute of Fisheries and Oceanography, Moscow, Russia) and Sergey Blokhin (Pacific Research Fisheries Center, Vladivostok, Russia) for providing photographs of *Eschrichtius robustus*; Lena Godlevska (Schmalhausen Institute of Zoology, National Academy of Sciences of Ukraine, Kiev, Ukraine) for assisting with the photography; Igor Dzeverin (Schmalhausen Institute of Zoology, National Academy of Sciences of Ukraine, Kiev, Ukraine) for discussing a draft of the manuscript; Robert Boessenecker (University of Otago, Dunedin, New Zealand) and Toshiyuki Kimura (Gunma Museum of Natural History, Tomioka, Japan) for their constructive reviews and improvements to the manuscript; and Felix Marx for editorial remarks. This study was partially supported by a Sepkoski Grant from the Paleontological Society International Research Program.

## References

- Arnold, P.W., Birtles, R.A., Soltzick, S., Matthews, M., and Dunstan, A. 2005. Gulp behavior in rorqual whales: underwater observations and functional interpretation. *Memoirs of the Queensland Museum* 51: 309–332.
- Beatty, B.L. and Dooley, A.C. 2009. Injuries in a mysticete skeleton from the Miocene of Virginia, with a discussion of buoyancy and the primitive feeding mode in the Chaemysticeti. *Jeffersoniana* 20: 1–28.
- Beauregard, H. 1882. L'articulation temporomaxillaire chez les Cétacés. *Journal de l'Anatomie et la Physiologie* 18: 16–26.
- Bisconti, M. 2006. *Titanocetus*, a new baleen whale from the Middle Miocene of northern Italy (Mammalia, Cetacea, Mysticeti). *Journal of Vertebrate Paleontology* 26: 344–364.
- Bisconti, M. 2008. Morphology and phylogenetic relationships of a new eschrichtiid genus (Cetacea: Mysticeti) from the Early Pliocene of northern Italy. *Zoological Journal of the Linnean Society* 153: 161–186.
- Bisconti, M. 2012. Comparative osteology and phylogenetic relationships of *Miocaperea pulchra*, the first fossil pygmy right whale genus and species (Cetacea, Mysticeti, Neobalaenidae). *Zoological Journal of the Linnean Society* 166: 876–911.
- Bock, W.J. 1964. Kinetics of the avian skull. *Journal of Morphology* 114: 1–42.
- Boessenecker, R.W. 2011. Herpetocetine (Cetacea: Mysticeti) dentaries from the Upper Miocene Santa Margarita Sandstone of Central California. *PaleoBios* 30: 1–12.
- Bouetel, V. 2005. Phylogenetic implications of skull structure and feeding in balaenopterids (Cetacea, Mysticeti). *Journal of Mammalogy* 86: 139–146.
- Bouetel, V. and Muizon, C. de 2006. The anatomy and relationships of *Piscobalaena nana* (Cetacea, Mysticeti), a Cetotheriidae s.s. from the early Pliocene of Peru. *Geodiversitas* 28: 319–395.
- Brandt, J.F. 1843. De Cetotherio, novo balaenarum familiae genere, in Rossia meridionali anti aliquot annos eff. oso. *Bulletin de l'Académie impériale des Sciences de St. Petersburg* (2) 1: 145–148.
- Brandt, J.F. 1871. Bericht über den Fortgang meiner Studien über die Cetaceen, welche das grosse zur Tertiärzeit von Mitteleuropa bis Centralasien hinein ausgedehnte Meeresbecken bevölkerten. *Bulletin de l'Académie Impériale de St. Petersburg* 16: 563–566.
- Brandt, J.F. 1872. Bericht über den bereits vollendeten, druckfertigen Theil meiner Untersuchungen über die fossilen und subfossilen Cetaceen Europas. *Compte rendu de l'Académie impériale des Sciences de St. Petersburg* 17: 407–408.
- Brandt, J.F. 1873. Untersuchungen über die fossilen und subfossilen Cetaceen Europas. *Memoires de l'Académie de St Petersburg* 20 (1), ser. 7: 1–371.
- Brisson, M.J. 1762. *Regnum animale in classes IX distributum, sive synopsis methodical sistens generalem animalium distributionem in classes IX, & duarum primarium classium, quadrupedum scilicet & cetaceorum, particularum divisionem in ordines, sectiones, genera, & species. Editio altera auctior [= Second edition]*. 296 pp. Theodorum Haak, Lugduni Batavorum, Leiden.
- Buchholtz, E.A. 2001. Vertebral osteology and swimming style in living and fossil whales (order: Cetacea). *Journal of Zoology, London* 253: 175–190.
- Buchholtz, E.A. 2007. Modular evolution of the Cetacean vertebral column. *Evolution and Development* 9: 278–289.
- Buchholtz, E.A. 2011. Vertebral and rib anatomy in *Caperea marginata*: Implications for evolutionary patterning of the mammalian vertebral column. *Marine Mammal Science* 27: 382–397.
- Buffrénil, V. de, Ricqlès, A. de, Ray, C.E., and Domning, D.P. 1990. Bone histology of the ribs of the archaeocetes (Mammalia: Cetacea). *Journal of Vertebrate Paleontology* 10: 455–466.
- Buffrénil, V. de, Canoville, A., D'Anastasio, R., and Domning, D.P. 2010. Evolution of sirenian pachyosteosclerosis, a model-case for the study of bone structure in aquatic tetrapods. *Journal of Mammalian Evolution* 17: 101–120.
- Capellini, G. 1901. Balenottera Miocenica del Monte Titano Repubblica di S. Marino. *Memorie della R. Accademia delle Scienze dell'Istituto di Bologna* 9: 1–26.
- Carte, A. and Macalister, A. 1868. On the anatomy of *Balaenoptera rosstrata*. *Philosophical Transactions of the Royal Society of London* 158: 201–261.
- Churchill, M., Berta, A., and Deméré, T. 2012. The systematics of right whales (Mysticeti: Balaenidae). *Marine Mammal Science* 28: 497–521.
- Cope, E.D. 1896. Sixth contribution to the knowledge of the Miocene fauna of North Carolina. *Proceedings of the American Philosophical Society* 35: 139–146.
- Dawson, M.M., Metzger, K.A., Baier, D.B., and Brainerd, E.L. 2011. Kinematics of the quadrate bone during feeding in Mallard ducks. *Journal of Experimental Biology* 214: 2036–2046.
- Deméré, T.A. and Berta, A. 2008. Cranial anatomy of the toothed mysticete *Aetiocetus weltoni* and its implications for aetiocetid phylogeny. *Zoological Journal of the Linnean Society* 154: 308–352.
- Ekdale, E.G., Berta, A., and Deméré, T.A. 2011. The comparative osteology of the petrotympanic complex (ear region) of extant baleen whales (Cetacea: Mysticeti). *PLoS ONE* 6 (6): e21311.
- El Adli, J. and Boessenecker, R.W. 2011. The musculature of the temporomandibular region in the Mio-Pliocene baleen [whale] genus *Herpetocetus* and its inference for feeding strategy. *Journal of Vertebrate Paleontology* 31: 104A.
- Fitzgerald, E.M.G. 2012. Possible neobalaenid from the Miocene of Australia implies a long evolutionary history for the pygmy right whale *Caperea marginata* (Cetacea, Mysticeti). *Journal of Vertebrate Paleontology* 32: 976–980.
- Fordyce, R.E. and Marx, F.G. 2012. The pygmy right whale *Caperea marginata*: the last of the cetotheres. *Proceedings of the Royal Society of London B* 280: 20122645.
- Galatius, A., Berta, A., Frandsen, M.S., and Goodall, R.N.P. 2011. Interspecific variation of ontogeny and skull shape among porpoises (Phocoenidae). *Journal of Morphology* 272: 136–148.
- Galatius, A. and Gol'din, P.E. 2011. Geographic variation of skeletal ontogeny and skull shape in the harbour porpoise (*Phocoena phocoena*). *Canadian Journal of Zoology* 89: 869–879.
- Goloboff, P.A., Farris, J.S., and Nixon, K.C. 2003. *T.N.T.: Tree Analysis Using New Technology*. Program and documentation available from the authors, and from [www.zmuc.dk/public/phylogeny/TNT](http://www.zmuc.dk/public/phylogeny/TNT)
- Gray, J.E. 1846. On the cetaceous animals. In: J. Richardson and F.E. Gray (eds.), *The Zoology of the Voyage of H.M.S. Erebus and Terror, Under the Command of Captain Sir James Clark Ross, R.N., F.R.S.*, 13–53. E.W. Janson, London.
- Gray, J.E. 1864. On the Cetacea which have been observed in the seas surrounding the British Islands. *Proceedings of the Scientific Meetings of the Zoological Society of London* 1864: 195–248.
- Gray, N.-M., Kainec, K., Madar, S., Tomko, L., and Wolfe, S. 2007. Sink or swim? Bone density as a mechanism for buoyancy control in early cetaceans. *Anatomical Record* 290: 638–653.
- Hofstein, I.D. 1948. Pachyostosis in fossil whales [in Ukrainian]. *Zbirnyk Prats z Paleontologii i Stratygrafii, Instytut Geologičnyh Nauk URSR* 1 (2): 65–75.
- Hofstein, I.D. 1965. Materials on fossil cetaceans from the Geological Museum of the USSR Academy of Sciences in Kiev [in Russian]. *Paleontologičeskij Sbornik Lvovskogo Gosudarstvennogo Universiteta* 1 (2): 25–29.
- Johnston, C. and Berta, A. 2011. Comparative anatomy and evolutionary history of suction feeding in cetaceans. *Marine Mammal Science* 27: 493–513.
- Kellogg, R. 1929. A new cetothere from southern California. *University of California Publications in Geological Sciences* 18: 449–457.
- Kellogg, R. 1931. Pelagic mammals of the Temblor Formation of the Kern River region, California. *Proceedings of the California Academy of Science* 19: 217–397.
- Kellogg, R. 1934a. A new cetothere from the Modelo Formation at Los Angeles, California. *Carnegie Institution of Washington* 447: 83–104.
- Kellogg, R. 1934b. The Patagonian fossil whalebone whale, *Cetotherium moreni* (Lydekker). *Carnegie Institution of Washington* 447: 64–81.

- Kellogg, R. 1940. On the cetotheres figured by Vandelli. *Boletim do Laboratorio Mineralogico e Geologico da Universidade de Lisboa* 3: 13–23.
- Kellogg, R. 1968. Fossil marine mammals from the Miocene Calvert Formation of Maryland and Virginia. *Bulletin of the United States National Museum* 247: 103–201.
- Kimura, T. 2002. Feeding strategy of an Early Miocene cetother from the Toyama and Akeyo Formations, central Japan. *Palaontological Record* 6: 179–189.
- Kimura, T. 2005. Evolution of feeding strategies in the Mysticeti [in Japanese]. *The Paleontological Society of Japan* 77: 14–21.
- Kimura, T. 2006. Feeding strategies and evolutionary history of the Mysticeti [in Japanese]. In: *Abstract of the Annual Meeting of the Society of Evolutionary Studies, Japan*, 39. National Olympic Memorial Youth Center, Tokyo.
- Kimura, T. 2008. Outline of fossil baleen whale assemblages of Japan [in Japanese]. *Journal of Fossil Research* 40: 107–111.
- Kimura, T. 2012. Evolutionary history of the cetaceans [in Japanese]. In: T. Murayama and T. Morisaka (eds.), *Wisdom of the Ketos—What Science Found out about Dolphins and Whales*, 67–87. Tokai University Press, Kanagawa.
- Kimura, T. and Hasegawa, Y. 2010. A new baleen whale (Mysticeti: Cetotheriidae) from the earliest late Miocene of Japan and a reconsideration of the phylogeny of cetotheres. *Journal of Vertebrate Paleontology* 30 (2): 577–591.
- Lambertsen, R.H. 1983. Internal mechanism of rorqual feeding. *Journal of Mammalogy* 64: 76–88.
- Lambertsen, R. H. and Hintz, R.J. 2004. Maxillomandibular cam articulation discovered in North Atlantic minke whale. *Journal of Mammalogy* 85: 446–452.
- Lambertsen, R.H., Ulrich, N., and Straley, J. 1995. Frontomandibular stay of Balaenopteridae; a mechanism for momentum recapture during feeding. *Journal of Mammalogy* 76: 877–899.
- Lilljeborg, W. 1861. Hvalben funna i jorden på Gräsön i Roslagen i Sverige. *Föredrag vid Naturforskaremotet i Köpenhamn* 1860: 599–616.
- Macleod, C., Reidenberg, J., Weller, M., Santos, M., Herman, J., Goold, J., and Pierce, G. 2007. Breaking symmetry: The marine environment, prey size, and the evolution of asymmetry in cetacean skulls. *Anatomical Record* 290: 539–545.
- Marx, F.G. 2011. The more the merrier? A large cladistic analysis of mysticetes, and comments on the transition from teeth to baleen. *Journal of Mammalian Evolution* 18: 77–100.
- Marx, F.G., Buono, M.R., and Fordyce, R.E. 2013. Juvenile morphology: A clue to the origins of the most mysterious of mysticetes? *Naturwissenschaften* (published online).
- McGowen, M.R., Spaulding, M., and Gatesy, J. 2009. Divergence date estimation and a comprehensive molecular tree of extant cetaceans. *Molecular Phylogenetics and Evolution* 53: 891–906.
- Mchedlidze, G.A. 1964. *Iskopaemye kitoobraznye Kavkaza*. 146 pp. Metsniereba, Tbilisi.
- Mchedlidze, G.A. 1970. *Nekotorye obšie herty istorii kittobraznyh*. 114 pp. Metsniereba, Tbilisi.
- Mead, J.G. and Fordyce, R.E. 2009. The therian skull: a lexicon with emphasis on the odontocetes. *Smithsonian Contributions to Zoology* 627: 1–248.
- Monteiro-Filho, E.L.D., Monteiro, L.R., and dos Reis, S.F. 2002. Skull shape and size divergence in dolphins of the genus *Sotalia*: a tridimensional morphometric analysis. *Journal of Mammalogy* 83: 125–134.
- Neveškaya, L.A., Goncharova, I.A., Ilyina, L.B., Paramonova, N.P., and Khondkarian, S.O. 2003. On the Neogene stratigraphic scale of the East Paratethys [in Russian]. *Stratigrafîa. Geologičeskaâ Korrelyaciâ* 11 (2): 3–26.
- Pilleri, G. and Siber, H.J. 1989. Neuer Spättertiärer cetotherid (Cetacea, Mysticeti) aus der Pisco-Formation Perus. In: G. Pilleri (ed.), *Beiträge zur Paläontologie der Cetaceen Perus*, 109–115. Hirnanatomisches Institut, Ostermündigen.
- Pivorunas, A. 1977. The fibrocartilage skeleton and related structures of the ventral pouch of balaenopterid whales. *Journal of Morphology* 151: 299–314.
- Radionova, E.P., Golovina, L.A., Filippova, N. Yu., Trubikhin, V.M., Popov, S.V., Goncharova, I.A., Vernigorova, Yu.V., and Pinchuk, T.N. 2012. Middle–Upper Miocene stratigraphy of the Taman Peninsula, Eastern Paratethys. *Central European Journal of Geosciences* 4: 188–204.
- Rathke, H. 1835. Ueber einige auf der Halbinsel Taman gefundene fossile Knochen. *Mémoires présentés à l'Académie Impériale des Sciences de St. Petersbourg par divers savans* 2: 331–336.
- Ray, G.C. and Schevill, W.E. 1974. Feeding of a captive gray whale, *Eschrichtius robustus*. *Marine Fisheries Review* 36: 31–38.
- Reidenberg, J.S. and Laitman, J.T. 1994. Anatomy of the hyoid apparatus in Odontoceti (toothed whales): Specializations of their skeleton and musculature compared with those of terrestrial mammals. *The Anatomical Record* 240: 598–624.
- Riabinin, A.I. [Râbinin, A.I.] 1934. New materials on the osteology of *Cetotherium mayeri* Brandt from the Upper Sarmatian of the Northern Caucasus [in Russian]. *Trudy Vsesoûznogo Geologorazvedochnogo Ob'edineniâ SSSR* 350: 1–15.
- Roth, F. 1978. *Mesocetus argillarius* sp. n. (Cetacea, Mysticeti) from Upper Miocene of Denmark, with remarks on the lower jaw and echolocation system in whale phylogeny. *Zoologica Scripta* 7: 63–79.
- Sanderson, S.L. and Wassersug, R. 1993. Convergent and alternative designs for vertebrate suspension feeding. In: J. Hanken and B.K. Hall (eds.), *The Skull. Volume 3*, 37–112. University of Chicago Press, Chicago.
- Sasaki, T., Nikaido, M., Hamilton, H., Goto, M., Kato, H., Kanda, N., Pastene, L.A., Cao, Y., Fordyce, R.E., Hasegawa, M., and Okada, N. 2005. Mitochondrial phylogenetics and evolution of mysticete whales. *Systematic Biology* 54: 77–99.
- Schulte, H.V.W. 1916. Monographs of the Pacific Cetacea. The Sei whale (*Balaenoptera borealis* Lesson). Part 2: Anatomy of a foetus of *Balaenoptera borealis*. *Memoirs of the American Museum of Natural History, New York* 1 (6), Part 1: 391–502.
- Spassky, P.I. [Spasskij, P.I.] 1954. Cetacean remains from Sarmatian deposits of Derbent environs [in Russian]. *Trudy Estestvenno-Istoričeskogo Muzeâ Imeni Zardabi, Baku* 8: 188–225.
- Steehan, M.E. 2007. Cladistic analysis and a revised classification of fossil and recent mysticetes. *Zoological Journal of the Linnean Society* 150: 875–894.
- Steehan, M.E. 2010. The extinct baleen whale fauna from the Miocene–Pliocene of Belgium and the diagnostic cetacean ear bones. *Journal of Systematic Palaeontology* 8: 63–80.
- Tarasenko, K.K. and Lopatin, A.V. 2012. New baleen whale genera (Cetacea, Mammalia) from the Miocene of the Northern Caucasus and Ciscaucasia: 1. *Kurdalagonus* gen. nov. from the Middle–Late Sarmatian of Adygea [in Russian]. *Paleontologičeskij žurnal* 5: 86–98.
- Tereshy, B.R. and Wiley, D.N. 1992. Asymmetrical pigmentation in the fin whale: a test of two feeding related hypotheses. *Marine Mammal Science* 8: 315–318.
- True, F. 1904. The whalebone whales of the western North Atlantic. *Smithsonian Contributions to Knowledge* 33: 1–332.
- Van Beneden, P.-J. 1859. Rapport de M. Van Beneden. *Bulletin de l'Académie Royale des Sciences, des Lettres et des Beaux-Arts de Belgique* 8: 123–146.
- Van Beneden, P.-J. 1872. Les baleines fossiles d'Anvers. *Bulletin de l'Académie Royale des Sciences, des Lettres et des Beaux-Arts de Belgique, Series 2* 40: 736–758.
- Vandelli, A.A. 1831. Additamentos ou notas a memoria geognostica ou golpe de vista do perfil das estratifi cacoes das diferentes rochas que compoem os terrenos desde a Serra de Cintra ate a de Arrabida. *Historia e memorias da Academia real das ciencias de Lisboa* 2 (1): 281–306.
- Werth, A.J. 2007. Adaptations of the cetacean hyolingual apparatus for aquatic feeding and thermoregulation. *Anatomical Record* 290: 546–568.
- Whitmore, F.C.J. and Barnes, L.G. 2008. Herpetocetinae, a new subfamily of extinct baleen whales (Mammalia, Cetacea, Cetotheriidae). *Virginia Museum of Natural History Special Publication* 14: 141–180.
- Woodward, B.L. and Winn, J.P. 2006. Apparent lateralized behavior in gray whales feeding off the central British Columbia coast. *Marine Mammal Science* 22: 64–73.
- Zweers, G.A. 1974. Structure, movement and myography of the feeding apparatus of the mallard (*Anas platyrhynchos* L.) a study in functional anatomy. *Netherlands Journal of Zoology* 24: 323–467.